Natural product-inspired esters and amides of ferulic and caffeic acid as dual inhibitors of HIV-1 reverse transcriptase

Vijay P. Sonar [a], *Angela Corona* [b], *Simona Distinto* [a], *Elias Maccioni* [a], *Rita Meleddu* [a], *Benedetta Fois* [a], *Costantino Floris* [c], *Nilesh V. Malpure* [d], *Stefano Alcaro* [e], *Enzo Tramontano* [b], *Filippo Cottiglia* [a,]*

[a] Department of Life and Environmental Sciences, Drug Sciences Section, University of Cagliari, via Ospedale 72, 09124 Cagliari, Italy

[b] Department of Life and Environmental Sciences, University of Cagliari, Cittadella di Monserrato SS554, 09042, Monserrato, Cagliari, Italy

[c] Dipartimento di Scienze Chimiche, University of Cagliari, Cittadella di Monserrato, 09042, Monserrato, Cagliari, Italy

[d] Department of Botany, S. S. G. M. College, IN-423601 Kopargaon, District Ahmednagar, MS, India

[e] Dipartimento di Scienze della Salute, Università "Magna Græcia" di Catanzaro, Campus "S. Venuta", Viale Europa, 88100 Catanzaro, Italy

*Corresponding author. Tel.: +39-706758979; fax: +39-706758553; e-mail: cottiglf@unica.it

Abstract

Using an HIV-1 Reverse Transcriptase (RT)-associated RNase H inhibition assay as lead, bioguided fractionation of the dichloromethane extract of the *Ocimum sanctum* leaves led to the isolation of five triterpenes (**1-5**) along with three 3-methoxy-4-hydroxy phenyl derivatives (**6-8**). The structure of this isolates were determined by 1D and 2D NMR experiments as well as ESI-MS. Tetradecyl ferulate (**8**) showed an interesting RNase H IC_{50} value of 12.4 μM and due to the synthetic accessibility of this secondary metabolite, a structure-activity relationship study was carried out. A series of esters and amides of ferulic and caffeic acids were synthesized and, among all, the most active was N-oleylcaffeamide displaying a strong inhibitory activity towards both RT-associated functions, ribonuclease H and DNA polymerase. Molecular modeling studies together with Yonetani-Theorell analysis, demonstrated that N-oleylcaffeamide is able to bind both two allosteric site located one close to the NNRTI binding pocket and the other close to RNase H catalytic site.

KEYWORDS. *Ocimum sanctum*, HIV-1, RNase H, reverse transcriptase, triterpenes, ferulic acid derivatives

ABBREVIATIONS. AIDS, Acquired Immunodeficiency Syndrome; DCM, dichloromethane; DMAP, 4-dimethylaminopyridine; DP, DNA polymerase; DQF-COSY, Double Quantum Filtered-COrrelation SpectroscopY; HAART, Highly Active Antiretroviral Therapy; HIV-1, human immunodeficiency virus type 1; HMBC, Heteronuclear Multiple Bond Correlation; HSQC, Heteronuclear Single Quantum Coherence spectroscopy; NNRTI, Non-Nucleoside RT Inhibitor; QMPL, Quantum Mechanic-Polarized Ligand; RDDP, RNA-dependent DNA polymerase; RNase H, ribonuclease H; RT, reverse transcriptase; TEA, triethylamine; VLC, vacuum-liquid chromatography.

1. Introduction

Acquired immunodeficiency syndrome (AIDS), caused by human immunodeficiency virus type 1 (HIV-1), represents the second most important cause of mortality in low-income countries and one of the ten leading cause of death worldwide. Although antiretroviral therapy has dramatically improved the outcome of HIV infection, it is not curative. Currently, the approved treatment of HIV infection and prevention on its progression towards AIDS is based on the highly active antiretroviral therapy (HAART) which combine at least two, and preferably three, antiviral agents, targeting different steps of the virus replication cycle [1]. Although the therapy has had considerable success in controlling HIV diffusion, there are associated adverse effects and emergence of multi-drug resistance [1, 2]. The majority of the 30 approved anti-AIDS drugs is represented by reverse transcriptase (RT) inhibitors. RT is the enzyme responsible for the conversion of the single-stranded RNA genome into a double-stranded DNA via the formation of a RNA-DNA hybrid. The RT is a multifunctional enzyme with DNA polymerase (DP) and ribonuclease H (RNase H) activities [3]. Despite the fact that both RT associated RNA-dependent DNA polymerase (RDDP) and RNase H functions are essential for viral replication [4,5] and have been explored as drug targets, all of the RT-targeting clinical approved drugs inhibit the polymerase activity [6]. Clearly, the development of compounds inhibiting both RT activities would have several advantages, leading to a complete block of RT functions, new favourable drug resistance profiles, reduction of combined drugs and of toxic side effects [7]. Various natural compounds are reported to inhibit RNase H function binding to the catalytic site, such as hydroxylated tropolones, illimaquinone, quercetin, and galloyl derivatives [8] and recently a natural compound, Sennoside A, derived from the traditional Chinese medicine plant *Rheum* L., has been reported to inhibit both HIV-1 RT-associated functions by an allosteric mode of action and to inhibit also viral replication [9], hence confirming the great potential of natural extract as a source of antiviral agents.

Ocimum sanctum L., known as “Tulsi” or “Holy Basil”, has been used in traditional Indian medicine and finds mention in the ancient Ayurvedic text *Charaka Samhita* [10]. Considered as a potent adaptogen, Tulsi has a unique combination of pharmacological actions that promote wellbeing and resilience [11]. *O. sanctum* has been used either alone or in combination with other medicinal plants to treat common colds, coughs, headaches, stomach disorders, inflammation, heart disease, various forms of poisoning, skin diseases, rheumatism and arthritis [11]. Some studies reported an anti-HIV activity of *O. sanctum* extracts alone or in combination with other plants in both *in vitro* and *in vivo* [12, 13] but, surprisingly, no phytochemical investigation has been done with the aim to identify the bioactive compound(s).

In our continuous search of biologically active secondary metabolites from plants [14], we selected a dichloromethane extract obtained from the leaves of *O. sanctum* that showed a good inhibitory activity towards HIV-1 RT-associated RNase H function. As consequence, in order to identify the antiviral compounds, a bioguided-fractionation of the extract was performed.

2. **Results and discussion**

2.1. *Isolation and characterization*

The dichloromethane extract of *O. sanctum* leaves, obtained by percolation, exhibited good HIV-1 RT-associated RNase H function inhibition with an IC_{50} of 4.2 μg/mL and therefore was fractionated by silica gel vacuum-liquid chromatography (VLC) to afford seven major fractions (F1-F7). All fractions were evaluated for their anti-RNase H activity (Table 1). Since F4-F7 showed significantly low IC_{50} values (2.4-4.0 μg/mL), they were subjected to purification by column chromatography (silica gel and Sephadex LH-20) and semi-preparative HPLC to afford four pentacyclic triterpenes, one sterol and three 3-methoxy-4-hydroxy phenyl derivatives.

Table 1. Effect of *O. sanctum* fractions on the HIV-1 RT-associated RNase H function

Fractions	RNase H
	[a]IC_{50} (μg/mL)
DCM extract	4.2 ± 0.9
F1	96 ± 5
F2	36 ± 6
F3	21 ± 0.1
F4	3.2 ± 0.1
F5	2.3 ± 0.3
F6	4 ± 1.5
F7	2.4 ± 0.3

[a]Extract concentration required to reduce the HIV-1 RT-associated RNase H activity by 50%.

Compounds **1**-**7** were identified as betulinic acid (**1**) [15], oleanolic acid (**2**) [16], ursolic acid (**3**) [16], pomolic acid (**4**) [17], stigmasterol (**5**) [18], vanillin (**6**) [19], and ferulaldehyde (**7**) [20] (Figure 1), by comparison of physical and spectroscopic data ($[\alpha]^{25}_{D}$, ^{1}H and ^{13}C NMR and MS) with those reported in the literature.

Compound **8** was obtained as a white semi-solid. The ^{1}H NMR spectrum showed a group of proton signals at 7.61 (d, J = 16.0 Hz, 1H), 7.07 (dd, J = 1.5, 8.0, 1H), 7.04 (d, br, 1H), 6.77 (d, J = 8.0 Hz, 1H), 6.29 (d, J = 16.0 Hz, 1H) and 3.93 (s, 3H) ppm, assignable to a feruloyl moiety. The cross-peak between the oxymethylene protons at 4.19 (t, J = 6.5 Hz, 2H) ppm and the carbonyl group at δ 167.7 observed in the Heteronuclear Multiple Bond Correlation (HMBC) spectrum, together with a cluster of aliphatic methylene groups (δ_H 1.26) and a terminal methyl (δ_H 0.88, t, J = 7.0 Hz 3H), indicated a ferulic acid long-chain alkyl ester. The length of the alkyl chain was unambiguously determined by ESI MS showing a molecular ion at 391 $[M+H]^+$. DQF-COSY, HSQC and HMBC experiments

allowed the complete assignments of all signals and the identification of compound **8** as tetradecyl ferulate [21].

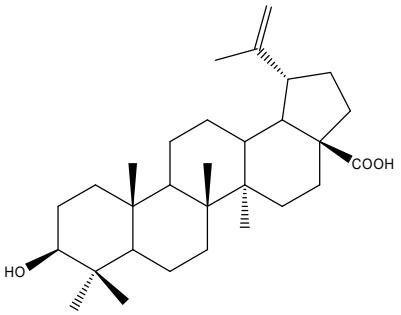

1

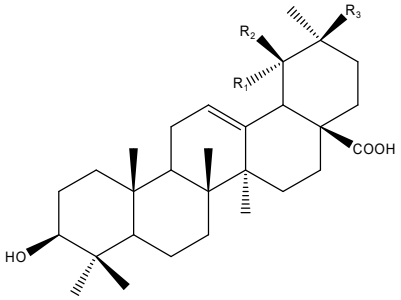

	R_1	R_2	R_3
2	H	H	CH_3
3	H	CH_3	H
4	OH	CH_3	H

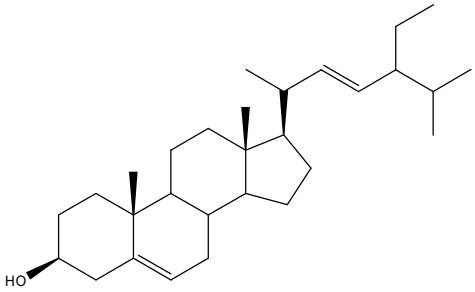

5

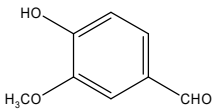

6

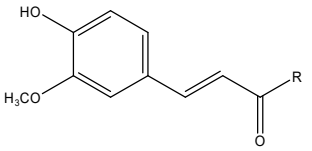

	R
7	H
8	$O(CH_2)_{13}CH_3$

Figure 1. Structures of the compounds isolated from *O. sanctum*

2.2 Synthesis

2.3 Synthesis of esters (**12b-l**) and amide (**13f**) of ferulic acid

The synthesis of ferulic acid esters **12b-l** was performed according to a previously described procedure [22] with some slight modifications, as illustrated in scheme 1.

Briefly, the reaction involved the synthesis of a mixed anhydride obtained by reaction of ferulic acid (**9**) and ethyl chloroformate in presence of TEA, at -15 °C. This step led to a simultaneous protection/activation of ferulic acid. The protected ferulic acid anhydride (**10**) was not isolated and the appropriate alcohol, in presence of catalytic amount of DMAP, was added to afford the protected esters (**11b-l**). The deprotection was easily achieved using excessive amounts of nucleophilic base (piperidine) at 0 °C, to give the expected esters (**12b-l**) in good yields. The amide **13f** was obtained adding excessive amounts of oleyl amine to the DCM solution of **10** giving, at once, amidation and deprotection (Scheme 1).

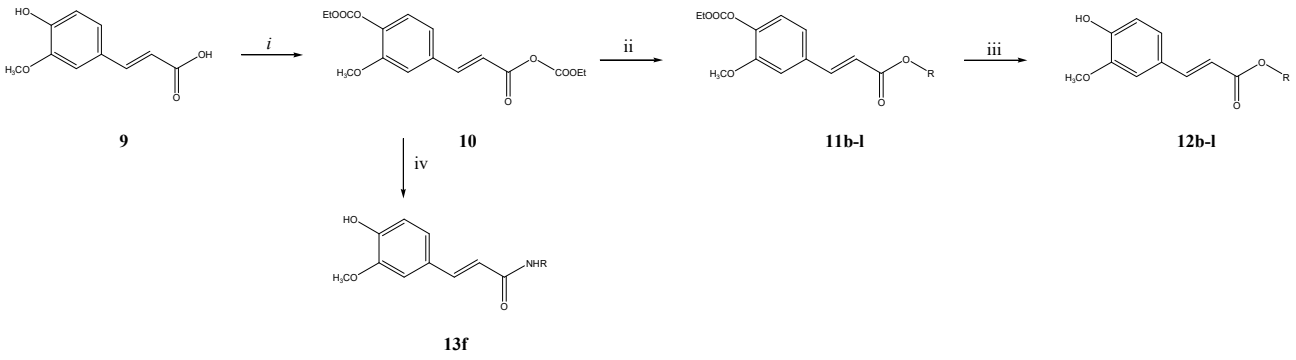

i: ClCOOEt, TEA, DCM, -15 °C, 1h; *ii*: ROH, DMAP, r.t.; *iii*: piperidine, 0 °C, 1h; *iv*: NH_2R, r.t.

Scheme 1. Synthetic pathway to compounds **12b-l** and **13f**

2.4 Synthesis of esters (**17f,g)** and amide (**18f**) of caffeic acid

The synthesis of esters (**17f,g**) and amide (**18f**) of caffeic acid was carried out using the same procedure of the ferulic acid esters but the protected caffeic acid mixed anhydride (**15**) was obtained by reaction of caffeic acid with 4.4 equivalents of ethyl chloroformate instead of 2.2 equivalents (Scheme 2).

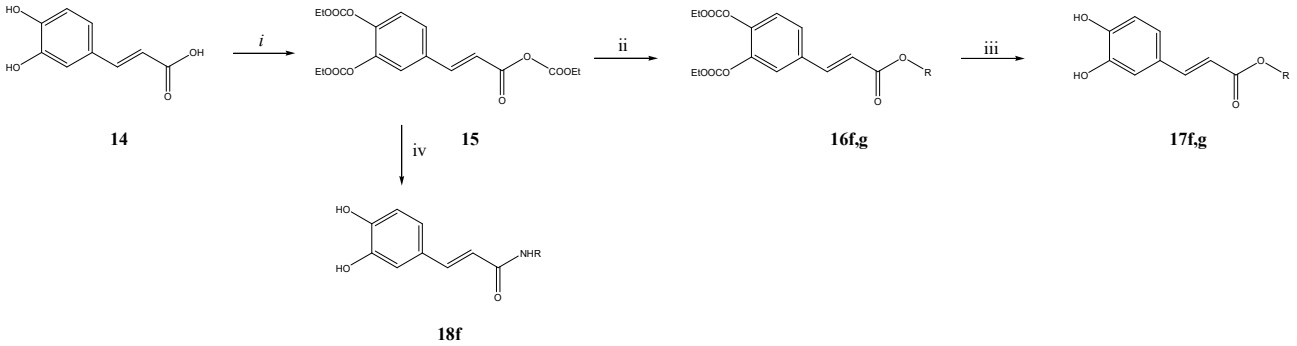

i: ClCOOEt, TEA, DCM, -15 °C, 1h; *ii*: ROH, DMAP, r.t.; *iii*: piperidine, 0 °C, 1h; *iv*: NH_2R, DMAP, r.t.

Scheme 2. Synthetic pathway to compounds **17f-g** and **18f**

2.5 Inhibitory effects on HIV-1 RT-associated functions and structure-activity relationships

The compounds isolated from the active fractions (F4-F7) of *O. sanctum* extract were evaluated for their anti-RNase H activity (Table 2) using as positive control RDS1759, a diketoacid inhibitor of the RNase H function that binds the catalytic site [23]. Among triterpenes, ursolic acid (**3**) was the most potent inhibitor with a IC_{50} value of 5.5 μM but also oleanolic acid (**2**) and pomolic acid (**4**) showed high potency with 7.5 and 9.3 μM, respectively. The substitution of the cyclohexane E ring with a cyclopentane, as in betulinic acid (**1**), reduced the potency and indicates the importance of the cyclohexane ring for the activity. Stigmasterol (**5**), containing a sterol skeleton, did not show any remarkable inhibitory activity with a IC_{50} of 153.3 μM. Among the 3-methoxy-4-hydroxy phenyl derivatives (**6-8**), tetradecyl ferulate (**8**) demonstrated an interesting anti-RNase H effect (IC_{50} 12.1 μM) whereas compounds **6** and **7**, possessing the same aromatic scaffold, did not show any RT inhibitory activity.

Table 2. Effect of the isolated and synthesized compounds on the HIV-1 RT-associated RNase H and RDDP functions

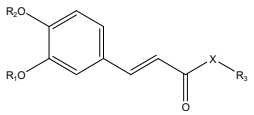

7-9, 12a-l, 13f, 16f-g, 17f-g, 18f

Compounds	R1	R2	R3	X	RNaseH [b]IC_{50} (µM)	RDDP [a]IC_{50} (µM)
Betulinic acid (1)	-	-	-	-	13.2 ± 1.9	[c]ND
Oleanolic acid (2)	-	-	-	-	7.5 ± 0.9	ND
Ursolic acid (3)	-	-	-	-	5.5 ± 0.3	ND
Pomolic acid (4)	-	-	-	-	9.3 ± 0.2	ND
Stigmasterol (5)	-	-	-	-	158.3 ± 7.8	ND
Vanillin (6)	-	-	-	-	>100	>100
7	CH_3	H	-	H	>100	>100
8	CH_3	H	*n*-tetradecyl	O	12.1 ± 1.1	>100
9	CH_3	H	H	O	>100	>100
12a	CH_3	H	ethyl	O	>100	>100
12b	CH_3	H	*n*-decyl	O	22.8 ± 1.7	25.1 ± 0.5
12c	CH_3	H	*n*-dodecyl	O	17.0 ± 1.7	18.2 ± 1.4
12d	CH_3	H	*n*-hexadecyl	O	23.9 ± 0.2	>100
12e	CH_3	H	*n*-octadecyl	O	26.9 ± 0.7	>100
12f	CH_3	H	oleyl	O	10.6 ± 0.3	23.6 ± 3.2
12g	CH_3	H	geranylgeranyl	O	8.4 ± 0.2	9.8 ± 0.5
12h	CH_3	H	2-phenylethyl	O	>100	>100
12i	CH_3	H	2-(p-methylphenyl)ethyl	O	84.0 ± 1	50.0 ± 2
12j	CH_3	H	2-(o-methylphenyl)ethyl	O	75.0 ± 1	78.0 ± 2
12k	CH_3	H	2-(p-chlorophenyl)ethyl	O	57.3 ± 3	70.0 ± 3
12l	CH_3	H	2-(1-naphthyl)ethyl	O	37.3 ± 6	27.0 ± 1
13f	CH_3	H	oleyl	NH	25.3 ± 3.7	11.3 ± 2.1
16f	$COOC_2H_5$	$COOC_2H_5$	oleyl	O	15.6 ± 0.8	18.2 ± 3.0
16g	$COOC_2H_5$	$COOC_2H_5$	geranylgeranyl	O	11.7 ± 1.9	12.2 ± 1.4
17f	H	H	oleyl	O	1.06 ± 0.17	1.6 ± 0.08
17g	H	H	geranylgeranyl	O	1.04 ± 0.12	1.5 ± 0.02
18f	H	H	oleyl	NH	0.68 ± 0.15	2.3 ± 0.07
Oleyl alcohol (19)	-	-	-	-	40.0 ± 5	53.0 ± 8
Geranylgeraniol (20)	-	-	-	-	39.0 ± 7	22.2 ± 8
EFV	-	-		-	ND	0.012 ± 0.03
RDS1759	-	-	-	-	10.1 ± 2.2	ND

[a] Compound concentration required to reduce the HIV-1 RT-associated RNase H activity by 50%.
[b] Compound concentration required to reduce the HIV-1 RT-associated RNAdependent DNA polymerase activity by 50%.
[c] ND, not done.

Although we reported for the first time the RNase H inhibitory activity of triterpenes **2**-**4**, they have been already demonstrated to possess anti HIV-1 RT effect [24] and various semi-synthetic triterpene derivatives are known as anti HIV maturation/fusion agents [25].

For this reason, we focused our attention on compound **8** for which, as far as we know, no biological studies have been reported, although there is an increasing interest in esters and amides of ferulic acid [26, 27]. In addition, the synthetic accessibility of ferulic acid derivatives increased their appeal as lead compounds for potential anti HIV-1 agents development. Thus, we firstly asked whether tetradecyl ferulate might inhibit also the HIV-1 RT-associated RDDP function using efavirenz as positive control (Table 2) but the assay revealed that compound **8** did not inhibit the RDDP activity (IC_{50} > 100 μM).

In order to find a structure-activity relationship, we decided to test the inhibitory activities of the commercially available ferulic acid (**9**) and ethyl ferulate (**12a**) against both RNase and RDDP functions. Both compounds did not display any activity *versus* the two RT-associated functions (Table 2). All these data led to the conclusion that the esterification of ferulic acid with a long alkyl chain is essential for the inhibition of RNase H function. Therefore, using saturated and unsaturated aliphatic alcohols, we decided to synthesize a series of ferulic acid esters (**12b-g**) (Scheme 1) and to evaluate their inhibition potency towards the two RT associated functions. The inhibitory activity of the RNase H function of the saturated 10C-18C alkyl ferulates changed only slightly, with the natural tetradecyl ferulate (**8**) being still the most active. As regards the anti RDDP activity, a relatively short chain of 10C-12C allowed the double inhibition of RT-associated activities, whereas a chain longer than 12C annulled the anti RDDP function of ferulates. The introduction of double bonds in long alkyl chain ferulates (**12f,g**), by reaction with oleyl alcohol or geranylgeraniol [28], permitted to regain the anti RDDP activity and to increase potency towards RNase H function. Considering the increase of activity achieved by substitution of unsaturated alkyl chain, we decided to modify the aromatic portion synthesizing esters of caffeic acid (**17f,g**) in which geranylgeranyl or oleyl chain was held constant. It was found that the replacement of methyl ether in oleyl ferulate (**12f**) and geranylgeranyl ferulate **(12g**) with a hydroxyl group resulted in a strong enhancement of potency towards both RNase H (10-fold in **17f** and 8-fold in **17g**) and RDDP (15-fold in **17f** and 7-fold in **17g**) functions. The importance of *o*-hydroxyl substitution was determined analyzing the anti-RNase

and anti RDDP activities of the oleyl- and geranylgeranyl 3,4-diethoxycarbonyloxy caffeate (**16f,g**). With respect to oleyl and geranylgeranyl caffeate, compounds **16f,g** showed a substantial loss of potency from 8 to 15 folds, suggesting the importance of free hydroxyl groups for the interactions with both RT functions.

Furthermore, to exclude the possibility that the inhibitory activity was only due to the fatty alcohols, oleyl alcohol (**19**) and geranylgeraniol (**20**) were assayed for their inhibiting capability towards the two RT-associated functions. The two fatty alcohols showed very low inhibiting activity underling the requirement of their esterification with ferulic or caffeic acid. Bioisosteric replacement of ester functionality in compounds **12f** and **17f** with an amide moiety resulted either in an increase or reduction of potency, depending on the amides. In fact, among all tested compounds, N-oleylcaffeamide (**18f**) showed the higher inhibitory activity towards RNase H function with a IC_{50} of 0.68 μM maintaining a potency *versus* RDDP function very close to that of oleyl caffeate **17f**. On the contrary, N-oleylferulamide (**13f**) resulted in substantial loss of potency toward the RT-associated RNase function (2.5-fold) when compared to oleyl ferulate (**12f**) while the RDDP inhibition increased of 2-fold. To explore whether the substitution of the alkyl chain with a lipophilic aromatic moiety might increase the potency of ferulates, a series of ferulic acid phenethyl esters (**12h-l**) were synthesized. Ferulic acid phenylethyl ester (**12h**) did not show any efficacy against the two RT functions up to 100 μM and its analogues substituted at the phenyl ring either with electron-withdrawing (**12k**) or with electron-releasing (**12i**,**j**) groups were only slightly active (Table 2). The replacement of the phenyl ring by a naphthyl group (**12l**) further enhanced the inhibitory activity towards both RT-associated function but the IC_{50} values were only moderate.

2.6 Molecular modeling studies

In order to gain a deeper understanding of the RT–ligand interactions docking experiments were carried out. To overcome the exponential problem inherent to flexible ligand docking methods, seven clustered conformations of the target were selected [29-31]. Furthermore, due to the high flexibility of the ligands we took into account the conformations within 5 kcal/mol from the global minimum conformation and among them the most diverse conformations (with different values of RMSD compared with the global minimum) were selected and subjected to ligand flexible docking experiments. In fact several studies highlighted the different possible conformation adopted by compounds with a large number of rotatable bonds [32, 33]. In addition, different evaluation of docking studies analysed the influence of starting 3D ligand conformation and the number of those initial conformations on final docking results. Generally using more structures results in better conformational space searching. This assumption has been shown to be more accurate in several comparative experiments [34]. Performing docking studies with different starting conformations when the ligand has a low number of rotatable bonds is not necessary but, with high flexible ligands, this can be an important issue. Indeed, the size of the conformational space to be sampled increases exponentially with ligand flexibility and the thoroughness of the sampling is important for the correct prediction of binding mode [35]. QM-Polarized Ligand (QMPL) [36] docking experiments were carried out. The same docking protocol was applied successfully in previous studies [30, 31]. Two favorable binding pockets were retrieved. One close to the polymerase catalytic site, the other below the RNase H catalytic site between the two subunit p66 and p51 (Figure 2) [30, 31].

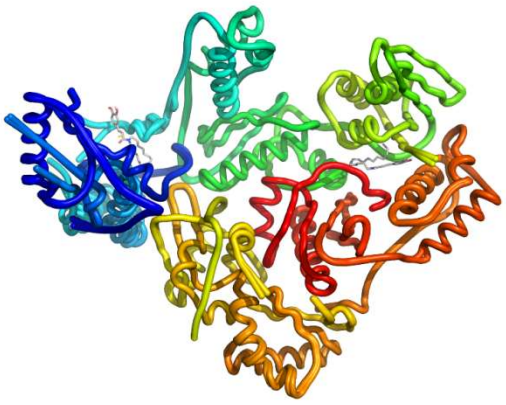

Figure 2. Superimposed minimized complexes **18f**-RT-HIV1. It is possible to see the two favourable binding pockets: one close to the NNRTI binding pocket and the other close to the RNAse H catalytic site.

Best docking complexes of the synthesized N-oleylcaffeamide (**18f**) were subjected to post- docking procedure based on energy minimization [30, 31]. In figure 3 it is clearly depicted how compound **18f** has the ability to harpoon the site discovered by Himmel as RNase allosteric site as well as the NNRTI [37]. This could lead to the inhibition of both RT HIV-1 catalytic activities. In fact, as hypothesized by Himmel, the compounds could be able to deviate the dsDNA-RNA preventing it binding to the RNase H catalytic site and, at the same time, they are able to interact with the NNRTI binding pocket locking the enzyme in a conformation that inhibits also its polymerase activity. Furthermore, docking experiments highlighted the possibility to bind also in another site below the RNase H catalytic site between the two subunits p66 and p51. The poses show the importance of the length of the chain and the possibility to be accommodated thanks to presence of the *cis* configured double bond. The geometry of the compound allows to enter the RNase H allosteric cavity which is narrow and long and with its optimal length is able to enter into the NNRTI binding pocket. The ligand enzyme complex is stabilized by hydrogen bond with Lys223 Tyr188, Leu 228 and hydrophobic interactions (green residues). The binding in the second site appears slightly less favored but could contribute to the inhibition of the RNAse H activity by deviating the trajectory of the nucleic acid. Similarly, in this case the complex is stabilized by hydrogen bond interactions (arrows) and hydrophobic interactions (green residues).

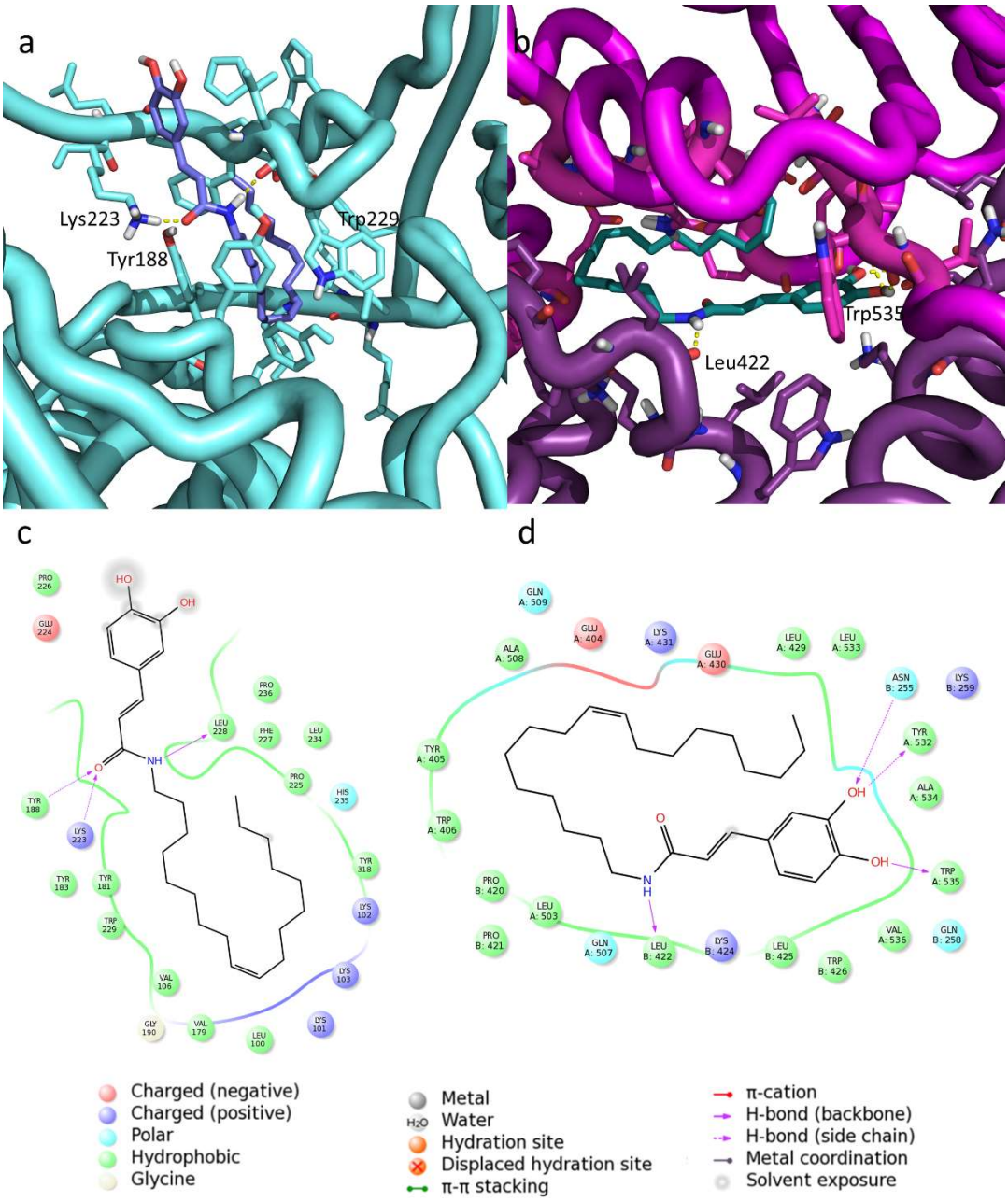

Figure 3. Putative binding mode of **18f**: a) in pocket 1; b) in pocket 2; c-d) respective 2D representation of compound and binding pocket interacting residues

2.7 The Yonetani-Theorell and Isobologram analysis

Hence, the molecular modelling studies indicated that amide **18f** inhibited the RNase H activity binding an allosteric site, despite its catechol moiety, potentially able to coordinate the Mg^{++} ions

within the RNase H catalytic site. In order to validate the docking poses, we firstly decided to verify the chelating potential of compound **18f** by measuring its UV spectrum of absorbance in the absence and in presence of $MgCl_2$, using the diketo acid derivative RDS1759 as positive control (Figure 4).

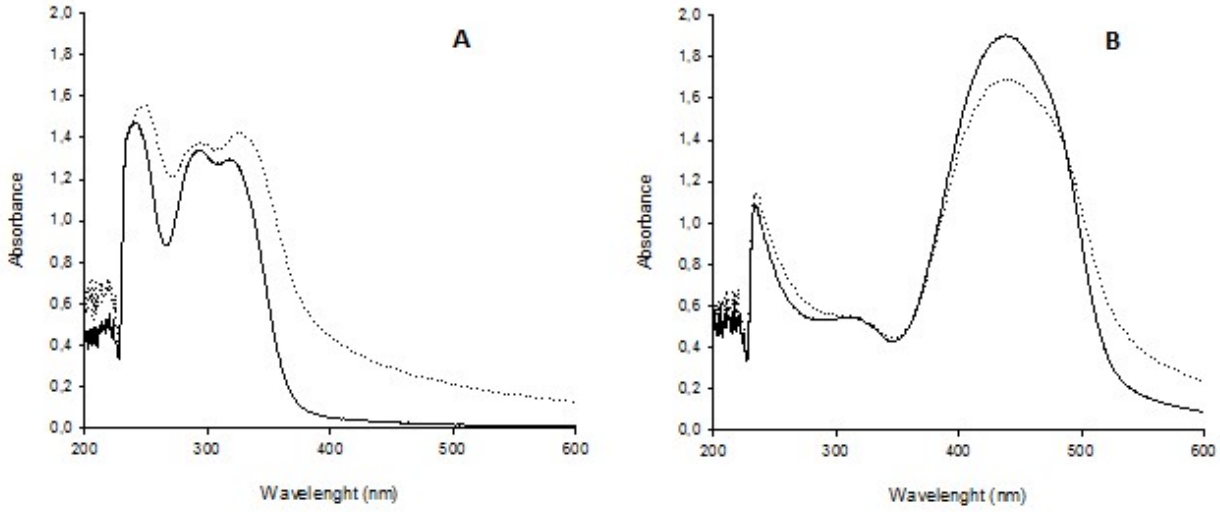

Figure 4. Effect of $MgCl_2$ on the spectrum of absorbance of compound **18f**. Chelation of Mg^{2+} by **18f** (panel A) and RDS1759 (panel B). UV–vis spectrum was measured with compound alone (unbroken line) or in the presence of 6 mM $MgCl_2$ (dotted line)

Results showed that **18f** maximum of absorbance shifted from 239 nm to 248 nm, in the presence of $MgCl_2$ suggesting the theoretical capability to chelate magnesium ions in the catalytic site of the RNase H function; however, the chelating capability is a necessary but not sufficient condition to bind the catalytic site. Hence, we further investigated the mode of action of compound **18f** with respect to RDS1759 by a revised Yonetani-Theorell analysis [38] on the combined effects of **18f** and RDS1759 on RNase H function. This model allows to discriminate between inhibitors that are

kinetically mutually exclusive (potentially competing for a single binding site) and inhibitors that are kinetically not mutually exclusive (potentially binding to non-overlapping sites). Results showed that the binding of compound **18f** is not kinetically mutually exclusive with RDS1759 for binding the catalytic site of the RNase H function, since in figure 5 we observed a series of intersected lines due to the binding of the two inhibitors to different enzyme sites (Figure 5, panel A). Furthermore, isobologram analysis (Figure 5, panel B) displayed a clear additive effect of the two compounds on the inhibition of HIV-1 RT-associated RNase H function.

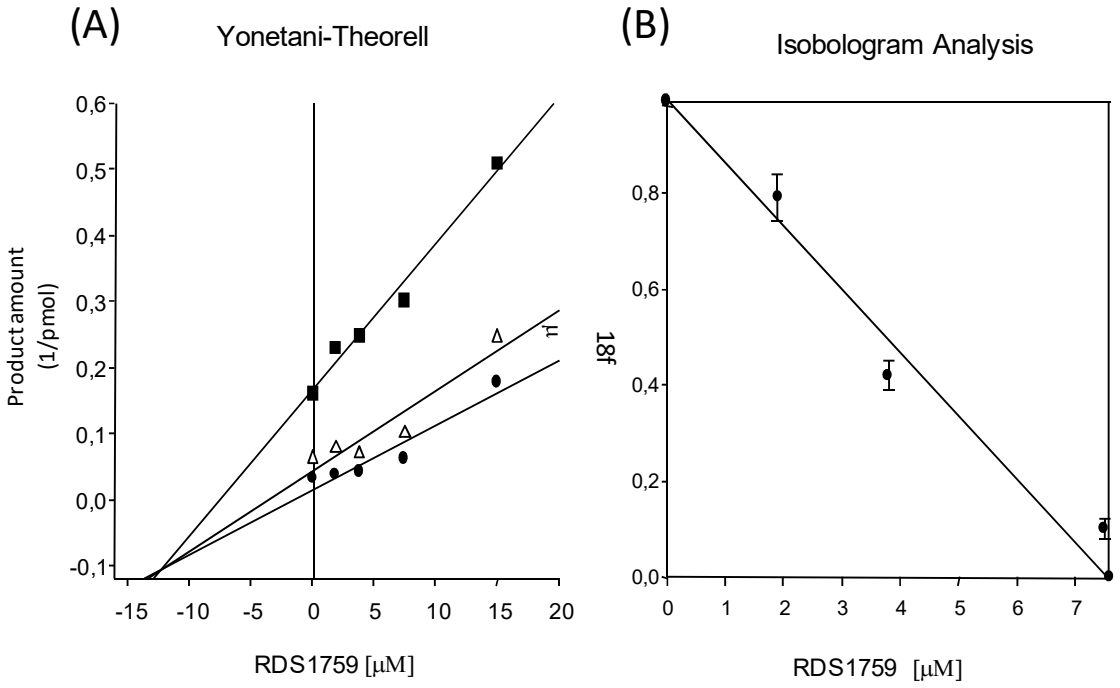

Figure 5. Panel A. Yonetani–Theorell analysis. Combination of **18f** and RDS1759 on the HIV-1 RT RNase H activity. HIVRT was incubated in the presence of RDS1759 alone (●) or combined with increasing concentrations of **18f** 1μM (Δ), 2 μM(■). Panel B. Isobologram analysis combination of compound **18f** and RDS1759 on the HIV-1 RT RNase H activity

3. Conclusion

In summary, we found that the anti-RT activity of the DCM extract is mainly due to the triterpenes ursolic, oleanolic and pomolic acids representing all together about the 0.5% of the extract and to a lesser extent to tetradecyl ferulate. These results could justify the antiretroviral activity of *O. sanctum* reported in previous work [12, 13]. More interestingly, our study permitted to discovery a natural HIV-1 RT-associated RNase H function inhibitor and a series of synthesized analogues with dual RT inhibition ability. Some compounds showed a strong potency towards both RT activities at low micromolar concentrations and, among all, N-oleylcaffeamide (**18f**) resulted as the most active. Moreover, molecular modelling studies, together with Yonetani-Theorell analysis, demonstrated that compound **18f** is able to bind both RNase allosteric site and NNRTI binding pocket. Thus, N-oleylcaffeamide and analogues may offer a new class of interesting HIV-1 RT inhibitor lead compounds for further optimization.

4. Experimental

4.1 General

Starting materials and reagents were obtained from commercial suppliers and were used without purification with the exception of geranylgeraniol that was isolated from *Otanthus maritimus* [28]. All melting points were determined on a Köfler apparatus and are uncorrected. Optical rotations were measured in $CHCl_3$ or MeOH at 25 °C using a Perkin-Elmer 241 polarimeter. UV spectra were recorded on a GBC Cintra 5 spectrophotometer. NMR spectra of all compounds except **12h-k** were recorded at 25 °C on Unity Inova 500NB high-resolution spectrometer (Agilent Technologies, CA, USA) operating at 500 MHz for ^{1}H and 100 MHz for ^{13}C, respectively. NMR spectra of compounds **12h-k** were measured on a Varian Unity INOVA 400 MHz spectrometer, operating at 400 MHz for ^{1}H and 100 MHz for ^{13}C, respectively. Compounds were measured in $CDCl_3$ and CD_3OD and the spectra referenced against residual non-deuterated solvents. ESIMS were measured on a AB Sciex

3200 QTrap LC-MS/MS triple quadrupole instrument. Column chromatography was carried out under TLC monitoring using silica gel (40-63 μm, Merck), and Sephadex LH-20 (25-100 μm, Pharmacia). For vacuum-liquid chromatography (VLC), silica gel (40-63 μm) (Merck) was used. TLC was performed on silica gel 60 F_{254} or RP-18 F_{254} (Merck). Semi-preparative HPLC was conducted by means of a Varian 920 LH instrument fitted with an autosampler module with a 1000 μL loop. The peak purities were monitored using a dual-wavelength UV detector settled at 254 and 366 nm. The columns were a 250 x 10 mm Spherisorb silica, particle size 5 μm (Waters) and a 250 x 10 mm Polaris C-18-A, particle size 5 μm (Varian). Elemental analyses were obtained on a Perkin Elmer 240 B microanalyzer. Analytical data of the synthesised compounds are in agreement within ± 0.4 % of the theoretical values.

4.2 Plant material

The aerial parts of *O. sanctum* were procured from Vedshree Ayurvedic Medical, Nasik, India and were authenticated by Prof. N. V. Malpure. A voucher specimen was deposited in the Herbarium of the Department of Life and Environmental Science, Drug Sciences Section, University of Cagliari.

4.3 Extraction and isolation

Air-dried and powdered leaves of *Ocimum sanctum* (500 g) were ground and extracted with CH_2Cl_2 (6 L) by percolation at room temperature to give 8.22 g dried extract. The CH_2Cl_2 extract was subjected to vacuum-liquid chromatography (VLC) (silica gel, 100 g, 40 - 63 μm) using a step gradient of *n*-hexane/CH_2Cl_2/EtOAc/MeOH (7.5 : 2.5 : 0 : 0 to 0 : 0 : 7.5 : 2.5, 300 mL each) to yield 7 main fractions (F1-F7). An aliquot of fraction F4 (2.50 g, eluted with CH_2Cl_2, 300 mL) was separated by column chromatography (CC) over silica gel using CH_2Cl_2/EtOAc (9.5 : 0.5) as eluent

to obtain eight subfractions (F4.1-F4.8). F4.5 (35 mg) was chromatographed by RP-HPLC using acetonitrile/H_2O (8.5:1.5, flow 2 mL/min) to give vanillin **6** (3.4 mg, t_R 7.1 min). F4.6 (32 mg) was treated with ACN and the insoluble portion resulted tetradecyl ferulate (**8**) (8.5 mg). The ACN soluble portion was purified by RP-HPLC using acetonitrile/H_2O (8.5:1.5, flow 2 mL/min) to yield vanillin **6** (2.3 mg, t_R 7.1 min). F4.7 (160 mg) was separated by CC on Sephadex LH-20 with MeOH as eluent to give two subfractions (F4.7.1-F4.7.2). F4.7.1 yielded stigmasterol (**5**) (28 mg) while F4.8.2 (9.0 mg) was further chromatographed by NP-HPLC using *n*-hexan/EtOAc (7:3, flow 2.3 mL/min) to give ferulaldehyde (**7**) (2.0 mg, t_R 13.0 min). An aliquot (20 mg) of F4.8 (1.20 g) was purified by RP-HPLC using MeOH/H_2O/trifluoroacetic acid (TFAA) (9.7:0.3:0.1, flow 2 mL/min) to yield oleanolic acid (**2**) (3.0 mg, t_R 11.5 min) and ursolic acid (**3**) (2.3 mg, t_R 12.5 min). F5 (840 mg), eluted with CH_2Cl_2/EtOAc (7.5 : 2.5, 300 mL), was subjected to column chromatography over silica gel to give six subfractions (F5.1-F5.6). F5.1 (80 mg) was purified by Sephadex LH-20 (MeOH) to give betulinic acid (**1**) (6.5 mg). An aliquot (50 mg) of F5.3 (210 mg) was subjected to RP-HPLC using MeOH/H_2O/trifluoroacetic acid (TFAA) (9.7:0.3:0.1, flow 2 mL/min) to yield pomolic acid (7.6 mg, t_R 8.5 min) and ursolic acid (4.6 mg, t_R 12.5 min). An aliquot (45 mg) of F5.6 (170 mg) was purified by RP-HPLC using MeOH/H_2O/trifluoroacetic acid (TFAA) (9.7:0.3:0.1, flow 2 mL/min) to yield oleanolic acid (**2**) (7.8 mg, t_R 11.5 min) and ursolic acid (**3**) (9.9 mg, t_R 12.5 min). Using the same condition described above, RP-HPLC analysis indicated that F6 (1.06 g) and F7 (1.58) contained a mixture of **2** and **3** in a ratio of about three to one.

4.4 General procedure for the synthesis of 4′-ethyloxycarbonyloxy ferulate **11b-l**

Ethyl chloroformate (0.76 mL, 8 mmol) and TEA (1.1 mL, 8 mmol) were added to a suspension of ferulic acid (0.737 g, 3.8 mmol) in DCM (10 mL) and stirred for 1 h at -15 °C until TLC analysis revealed a total consumption of starting material. Alcohol (8 mmol) and DMAP (0.030 g, 0.08 mmol) were then added and the mixture stirred at room temperature for 6 h. The solvent was evaporated

under reduced pressure to afford the crude product. This product was purified by silica gel column chromatography using mixtures of *n*-hexane/ethyl acetate or toluene/ethyl acetate as eluents.

4.4.1 *(E)-4-Ethyloxycarbonyloxy-3-methoxy decyl cinnamate (**11b**)*. White solid, yield: 73%; column chromatography mobile phase: toluene/ethyl acetate (9.5 : 0.5); ^{1}H NMR (500 MHz, $CDCl_3$): δ_H 7.63 (d, 1H, *J* = 16 Hz, H-3), 7.01 (m, 3H, H-2′, H-5′, H-6′), 6.38 (d, 1H, *J* = 16 Hz, H-2), 4.32 (q, 2H, *J* = 7.5 Hz, O$\underline{CH_2}$-CH_3), 4.19 (t, 2H, *J* = 6.8 Hz, H-1″), 3.87 (s, 3H, OCH_3-3′), 1.69 (m, 2H, H-2″), 1.39 (t, 3H, *J* = 7.5 Hz, OCH_2-$\underline{CH_3}$), 1.39 (m, 2H, H-3″), 1.25 (m, 12H, H-4″-H-9″), 0.87 (t, 3H, *J* = 6.8, Hz, H-10″).

4.4.2 *(E)-4-Ethyloxycarbonyloxy-3-methoxy dodecyl cinnamate (**11c**)*. White semi-solid, yield: 75%; column chromatography mobile phase: toluene/ethyl acetate (9.5 : 0.5); ^{1}H NMR (500 MHz, $CDCl_3$): δ_H 7.63 (d, 1H, *J* = 16 Hz, H-3), 7.03 (m, 3H, H-2′, H-5′, H-6′), 6.38 (d, 1H, *J* = 16 Hz, H-2), 4.33 (q, 2H, *J* = 7.5 Hz, O$\underline{CH_2}$-CH_3), 4.19 (t, 2H, *J* = 6.8 Hz, H-1″), 3.89 (s, 3H, OCH_3-3′), 1.69 (m, 2H, H-2″), 1.36 (t, 3H, *J* = 7.5 Hz, OCH_2-$\underline{CH_3}$), 1.35 (m, 2H, H-3″), 1.26 (m, 16H, H-4″-H-11″), 0.87 (t, 3H, *J* = 6.8, Hz, H-12″).

4.4.3 *(E)-4-Ethyloxycarbonyloxy-3-methoxy esadecyl cinnamate (**11d**)*. White solid, yield, 70%; column chromatography mobile phase: toluene/ethyl acetate (9.5 : 0.5); ^{1}H NMR (500 MHz, $CDCl_3$): δ_H 7.64 (d, 1H, *J* = 16 Hz, H-3), 7.02 (m, 3H, H-2′, H-5′, H-6′), 6.32 (d, 1H, *J* = 16 Hz, H-2), 4.32 (q, 2H, *J* = 7.5 Hz, O$\underline{CH_2}$-CH_3),4.20 (t, 2H, *J* = 6.8 Hz, H-1″), 3.89 (s, 3H, OCH_3-3′), 1.67 (m, 2H, H-2″), 1.39 (t, 3H, *J* = 7.5 Hz, OCH_2-$\underline{CH_3}$), 1.36 (m, 2H, H-3″), 1.26 (m, 24H, H-4″-H-15″), 0.88 (t, 3H, *J* = 6.8, Hz, H-16″).

4.4.4 (*E*)-*4-Ethyloxycarbonyloxy-3-methoxy octadecyl cinnamate (**11e**)*. White solid, yield: 79%; column chromatography mobile phase: toluene/ethyl acetate (9.5 : 0.5); ^{1}H NMR (500 MHz, $CDCl_3$): δ_H 7.62 (d, 1H, *J* = 16 Hz, H-3), 7.10 (m, 3H, H-2′, H-5′, H-6′), 6.37 (d, 1H, *J* = 16 Hz, H-2), 4.30 (q, 2H, *J* = 7.5 Hz, O$\underline{CH_2}$-CH_3),4.19 (t, 2H, *J* = 6.8 Hz, H-1″), 3.86 (s, 3H, OCH_3-3′), 1.69 (m, 2H, H-2″), 1.37 (t, 3H, *J* = 7.5 Hz, OCH_2-$\underline{CH_3}$), 1.36 (m, 2H, H-3″), 1.25 (m, 28H, H-4″-H-17″), 0.87 (t, 3H, *J* = 6.8, Hz, H-18″).

4.4.5 (*E*)-*4-Ethyloxycarbonyloxy-3-methoxy oleyl cinnamate (**11f**)*. White solid, yield: 68%; column chromatography mobile phase: toluene/ethyl acetate (9.5 : 0.5); ^{1}H NMR (500 MHz, $CDCl_3$): δ_H 7.65 (d, 1H, *J* = 16 Hz, H-3), 7.14 (m, 3H, H-2′, H-5′, H-6′), 6.41 (d, 1H, *J* = 16 Hz, H-2), 5.38 (m, 2H, H-9″, H-10″), 4.32 (q, 2H, *J* = 7.5 Hz, O$\underline{CH_2}$-CH_3), 4.2 (t, 2H, *J* = 6.8 Hz, H-1″), 3.87 (s, 3H, OCH_3-3′), 2.10 (4H, H-8″, H11″), 1.80 (m, 2H, H-2″), 1.39 (t, 3H, *J* = 7.5 Hz, OCH_2-$\underline{CH_3}$), 1.34 (m, 2H, H-3″), 1.26 (m, 4H, H-4″-H-5″), 1.29 (18H, H-6″, H-7″, H-12″-H-17″), 0.9 (t, 3H, *J* = 6.8, Hz, H-18″);

4.4.6 (*E*)-*4-Ethyloxycarbonyloxy-3-methoxy-O-geranylgeranyl cinnamate (**11g**)*. White solid yield: 70 %; column chromatography mobile phase: toluene/ethyl acetate (9.5 : 0.5); ^{1}H NMR (500 MHz, $CDCl_3$): δ_H 7.63 (d, 1H, *J* = 16 Hz, H-3), 7.13 (br s, 1H, H-2′), 7.09 (m, 2H, H-5′, H-6′), 6.39 (d, 1H, *J* = 16 Hz, H-2), 5.43 (t, 2H, *J* = 7.0 Hz, H-2″), 5.09 (m, 1H, H-14″), 5.07 (4H, m, H-6″, H-10″), 4.70 (d, 2H, *J* =7.5 Hz, H-1″), 4.31 (q, 2H, *J* = 7.5 Hz, O$\underline{CH_2}$-CH_3), 3.87 (s, 3H, OCH_3-3′), 2.16 (m, 2H, H-4″), 2.11(m, 2H, H-8″), 2.06 (m, 2H, H-12″), 1.98 (m, 6H, H-5″, H-9″, H-13″), 1.79 (s, 3H, H-20″), 1.67 (s, 3H, H-17″), 1.62 (s, 3H, H-16″), 1.59 (s, 6H, H-18″, H-19″), 1.38 (t, 3H, *J* = 7.5 Hz, OCH_2-$\underline{CH_3}$).

4.4.7 *2-Phenylethyl (E)-4-ethyloxycarbonyloxy-3-methoxy cinnamate (**11h**)*. White solid, yield: 79 %; column chromatography mobile phase: *n*-hexane/ethyl acetate (7 : 3); ^{1}H NMR (500 MHz,

$CDCl_3$): δ_H 7.70 (d, 1H, *J* = 15.6 Hz, H-3), 7.36 (m, 5H, H-4″-H8″), 7.2 (m, 3H, H-2′, H-5′, H-6′), 6.44 (d, 1H, *J* = 15.6 Hz, H-2), 4.51 (t, 2H, *J* = 6.8 Hz, H-1″), 4.39 (q, 2H, *J* = 7.5 Hz, O$\underline{CH_2}$-CH_3), 4.0 (s, 3H, OCH_3-3′), 3.10 (t, 2H, *J* = 6.8 Hz, H-2″), 1.46(t, 3H, *J* = 7.5 Hz, OCH_2-$\underline{CH_3}$).

4.4.8 *2-(p-Methyl-phenyl)ethyl (E)-4-ethyloxycarbonyloxy-3-methoxy cinnamate (**11i**)*. White solid, yield: 76 %; column chromatography mobile phase: *n*-hexane/ethyl acetate (8.5 : 1.5); ^{1}H NMR (500 MHz, $CDCl_3$): δ_H 7.63 (d, 1H, *J* = 15.6 Hz, H-3), 7.15 (m, 7H, H-2′, H-5′, H-6′, H-4″-H-5″, H-7″, H8″), 6.39 (d, 1H, *J* = 15.6 Hz, H-2), 4.42 (t, 2H, *J* = 6.8 Hz, H-1″), 4.33 (q, 2H, *J* = 7.5 Hz, O$\underline{CH_2}$-CH_3), 3.88 (s, 3H, OCH_3-3′), 2.99 (t, 2H, *J* = 6.8 Hz, H-2″), 2.34 (s, 3H, CH_3-6″), 1.39 (t, 3H, *J* = 7.5 Hz, OCH_2-$\underline{CH_3}$).

4.4.9 *2-(o-Methylphenyl)ethyl (E)-4-ethyloxycarbonyloxy-3-methoxy cinnamate (**11j**)*. White solid, yield: 79 %; column chromatography mobile phase: *n*-hexane/ethyl acetate (8.5 : 1.5); ^{1}H NMR (500 MHz, $CDCl_3$): δ_H 7.64 (d, 1H, *J* = 15.6 Hz, H-3), 7.16 (m, 7H, H-2′, H-5′, H-6′, H-5″-H8″), 6.38 (d, 1H, *J* = 15.6 Hz, H-2), 4.40 (t, 2H, *J* = 7 Hz, H-1″), 4.32 (q, 2H, *J* = 7.5 Hz, O$\underline{CH_2}$-CH_3), 3.89 (s, 3H, OCH_3-3′), 3.03 (t, 2H, *J* = 7 Hz, H-2″), 2.39 (s, 3H, CH_3-4″), ″), 1.39 (t, 3H, *J* = 7.5 Hz, OCH_2-$\underline{CH_3}$).

4.4.10 *2-(p-Chlorophenyl)ethyl (E)-4-ethyloxycarbonyloxy-3-methoxy cinnamate (**11k**)*. White solid, yield: 80 %; column chromatography mobile phase: *n*-hexane/ethyl acetate (8.5 : 1.5); ^{1}H NMR (500 MHz, $CDCl_3$): δ_H 7.58 (d, 1H, *J* = 16 Hz, H-3), 7.27 (d, 2H, *J* = 8 Hz, H-5″, H-7″), 7.16 (d, 2H, *J* = 8 Hz, H-4″, H-8″), 7.08 (m, 2H, H-2′, H-6′), 7.12 (d, 1H, *J* = 8 Hz, H-5′), 6.32 (d, 1H, *J* = 16 Hz, H-2), 4.38 (t, 2H, *J* = 6.8 Hz, H-1″), 4.29 (q, 2H, *J* = 7.5 Hz, O$\underline{CH_2}$-CH_3), 3.90 (s, 3H, OCH_3-3′), 2.96 (t, 2H, *J* = 6.8 Hz, H-2″), 1.36 (t, 3H, *J* = 7.5 Hz, OCH_2-$\underline{CH_3}$).

4.4.11 *2-(1-Naphthyl)ethyl (E)-4-ethyloxycarbonyloxy-3-methoxy cinnamate (**11l**)*. White solid, yield: 80 %; column chromatography mobile phase: *n*-hexane/ethyl acetate (8 : 2); ^{1}H NMR (500 MHz, $CDCl_3$): δ_H 8.15 (d, 1H, *J* = 8.5 Hz, H-11″), 7.88 (br d, 1H, *J* = 8 Hz, H-8″), 7.78 (br d, 1H, *J* = 7 Hz, H-6″), 7.61 (d, 1H, *J* = 16 Hz, H-3), 7.57 (m, 1H, H-10″), 7.50 (m, 1H, H-9″), 7.42 (m, 2H, H-4″,H-5″), 7.1 (m, 2H, H-2′, H-6′), 7.16 (d, 1H, *J* = 8, Hz, H-5′), 6.37 (d, 1H, *J* = 16 Hz, H-2), 4.57 (t, 2H, *J* = 7.5 Hz, H-1″), 4.33(q, 2H, *J* = 7.5 Hz, O$\underline{CH_2}$-CH_3), 3.89 (s, 3H, OCH_3-3′), 3.51 (t, 2H, *J* = 7.5 Hz, H-2″), 1.40 (t, 3H, *J* = 7.5 Hz, OCH_2-$\underline{CH_3}$).

4.5 General procedure for the synthesis of ferulate **12b-l**

To a solution of the each protected feruloyl ester **11b-l** (2.5 mmol) in DCM (10 mL) was added 80 equiv of piperidine (80 mmol) at 0 °C, and the reaction mixture was stirred at room temperature for 3h. The feruloyl ester was purified by VLC (silica gel) or Sephadex LH-20.

4.5.1 *Decyl ferulate (**12b**)*. White semi-solid, yield: 51%; VLC mobile phase: toluene/ethyl acetate (9.5 : 0.5); ^{1}H NMR (500 MHz, $CDCl_3$): δ_H 7.60 (d, 1H, *J* = 16 Hz, H-3), 7.06 (dd, 1H, *J* = 1.6, 8 Hz, H-6′), 7.02 (d, 1H, *J* = 1.6, Hz, H-2′), 6.90 (d, 1H, *J* = 8, Hz, H-5′), 6.28 (d, 1H, *J* = 16 Hz, H-2), 4.18 (t, 2H, *J* = 6.8 Hz, H-1″), 3.90 (s, 3H, OCH_3-3′), 1.69 (m, 2H, H-2″), 1.39 (m, 2H, H-3″), 1.25 (m, 12H, H-4″-H-9″), 0.87 (t, 3H, *J* = 6.8, Hz, H-10″); ^{13}C NMR (100 MHz, $CDCl_3$): δ_C 167.4 (C-1), 148.0 (C-3′), 146.9 (C-4′), 144.6 (C-3), 126.9 (C-1′), 122.9 (C-6′), 115.5 (C-2), 114.8 (C-5′), 109.4 (C-2′), 64.5 (C-1″), 55.8 (OCH_3), 31.8 (C-8″), 29.5 (C-5″ and C-6″), 29.2 (C-4″, C-7″), 28.7 (C-2″), 25.9 (C-3″), 22.6 (C-9″), 14.0 (C-10″); ESI mass (negative mode): 333 $[M - H]^-$, 375 $[M + ACN]^-$.

4.5.2 Do*decyl ferulate (**12c**)*. White solid, yield: 60%; m. p.: 55-56 °C; VLC mobile phase: toluene/ethyl acetate (9.5 : 0.5); ^{1}H NMR (500 MHz, $CDCl_3$): δ_H 7.60 (d, 1H, *J* = 16 Hz, H-3), 7.06 (dd, 1H, *J* = 1.6, 8 Hz, H-6′), 7.02 (d, 1H, *J* = 1.6, Hz, H-2′), 6.90 (d, 1H, *J* = 8, Hz, H-5′), 6.05 (s, 1H, OH), 6.28 (d, 1H, *J* = 16 Hz, H-2), 4.18 (t, 2H, *J* = 6.8 Hz, H-1″), 3.90 (s, 3H, OCH_3-3′), 1.69 (m, 2H, H-2″), 1.38 (m, 2H, H-3″), 1.26 (m, 16H, H-4″-H-11″), 0.87 (t, 3H, *J* = 6.8, Hz, H-12″); ^{13}C NMR (100 MHz, $CDCl_3$): δ_C 167.4 (C-1), 147.9 (C-3′), 146.8 (C-4′), 144.6 (C-3), 127.0 (C-1′), 123.0 (C-6′), 115.2 (C-2), 114.7 (C-5′), 109.3 (C-2′), 64.6 (C-1″), 55.9 (OCH_3), 31.9 (C-10″), 29.6, 29.5, 29.4, (C-5″- C-9″), 29.3 (C-4″), 28.7 (C-2″), 25.9 (C-3″), 22.6 (C-11″), 14.1 (C-12″); ESI mass (negative mode): 361 $[M-H]^-$, 403 $[M + ACN]^-$.

4.5.3 *Hexadecyl ferulate (**12d**)*. White solid, yield: 65%; m. p.: 57-59 °C; VLC mobile phase: toluene/ethyl acetate (9.5 : 0.5); ^{1}H NMR (500 MHz, $CDCl_3$): δ_H 7.61 (d, 1H, *J* = 16 Hz, H-3), 7.07 (dd, 1H, *J* = 1.6, 8 Hz, H-6′), 7.03 (d, 1H, *J* = 1.6, Hz, H-2′), 6.91(d, 1H, *J* = 8, Hz, H-5′), 6.29 (d, 1H, *J* = 16 Hz, H-2), 5.90 (s, 1H, OH), 4.19 (t, 2H, *J* = 6.8 Hz, H-1″), 3.92 (s, 3H, OCH_3-3′), 1.69 (m, 2H, H-2″), 1.39 (m, 2H, H-3″), 1.26 (m, 24H, H-4″-H-15″), 0.88 (t, 3H, *J* = 6.8, Hz, H-16″); ^{13}C NMR (100 MHz, $CDCl_3$): δ_C 167.3 (C-1), 147.9 (C-3′), 146.8 (C-4′), 144.6 (C-3), 127.1 (C-1′), 123.0 (C-6′), 115.7 (C-2), 114.7 (C-5′), 109.3 (C-2′), 64.6 (C-1″), 55.9 (OCH_3), 31.9 (C-14″), 29.7, 29.6, 29.5, (C-5″- C-12″), 29.4 (C-13″), 29.3 (C-4″), 28.8 (C-2″), 26.0 (C-3″), 22.7 (C-15″), 14.1 (C-16″); ESI mass (negative mode): 417 $[M-H]^-$, 459 $[M + ACN]^-$.

4.5.4 *Octadecyl ferulate. (**12e**)*. White solid, yield: 63 %; m. p.: 61-62 °C; VLC mobile phase: toluene/ethyl acetate (9.5 : 0.5); ^{1}H NMR (500 MHz, $CDCl_3$): δ_H 7.61 (d, 1H, *J* = 16 Hz, H-3), 7.07 (dd, 1H, *J* = 1.6, 8 Hz, H-6′), 7.03 (d, 1H, *J* = 1.6, Hz, H-2′), 6.91 (d, 1H, *J* = 8, Hz, H-5′), 6.29 (d, 1H, *J* = 16 Hz, H-2), 5.94 (s, 1H, OH), 4.19 (t, 2H, *J* = 6.8 Hz, H-1″), 3.92 (s, 3H, OCH_3-3′), 1.69

(m, 2H, H-2″), 1.40 (m, 2H, H-3″), 1.26 (m, 28H, H-4″-H-17″), 0.88 (t, 3H, *J* = 6.8, Hz, H-18″); ^{13}C NMR (100 MHz, $CDCl_3$): δ_C 167.3 (C-1), 147.9 (C-3′), 146.8 (C-4′), 144.6 (C-3), 127.1 (C-1′), 123.0 (C-6′), 115.7 (C-2), 114.7 (C-5′), 109.3 (C-2′), 64.6 (C-1″), 55.9 (OCH_3), 31.9 (C-16″), 29.7, 29.6, 29.5 (C-5″- C-14″), 29.4 (C-15″), 29.3 (C-4″), 28.8 (C-2″), 26.0 (C-3″), 22.7 (C-17″), 14.1 (C-18″); ESI mass (negative mode): 445 $[M-H]^-$, 487 $[M + ACN]^-$.

4.5.5 *Oleyl ferulate (**12f**)*. White solid, yield: 68 %; m. p.: 35-36 °C; VLC mobile phase: toluene/ethyl acetate (9.5 : 0.5); ^{1}H NMR (500 MHz, $CDCl_3$): δ_H 7.59 (d, 1H, *J* = 16 Hz, H-3), 7.03 (dd, 1H, *J* = 1.6, 8 Hz, H-6′), 6.97 (d, 1H, *J* = 1.6, Hz, H-2′), 6.91 (d, 1H, *J* = 8, Hz, H-5′), 6.27 (d, 1H, *J* = 16 Hz, H-2), 5.34 (m, 2H, H-9″, H-10″), 4.18 (t, 2H, *J* = 6.8 Hz, H-1″), 3.86 (s, 3H, OCH_3-3′), 2.0 (4H, H-8″, H11″), 1.68 (m, 2H, H-2″), 1.29 (m, 2H, H-3″), 1.26 (m, 4H, H-4″-H-5″), 1.25 (16H, H-6″, H-7″, H-12″-H-17″), 0.87 (t, 3H, *J* = 6.8, Hz, H-18″); ^{13}C NMR (100 MHz, $CDCl_3$): δ_C 167.3 (C-1), 148.0 (C-3′), 146.8 (C-4′), 144.6 (C-3), 129.8 (C-10″), 129.6 (C-9″), 126.8 (C-1′), 122.8 (C-6′), 115.4 (C-2), 114.7 (C-5′), 109.4 (C-2′), 64.5 (C-1″), 55.7 (OCH_3), 31.8 (C-16″), 29.7, 29.6, 29.4, 29.3, 29.2, 29.1, 29.0 (C-4″-C-7″, C-12″- C-15″), 28.7 (C-2″), 27.1 (C-8″, C-11″), 26.0 (C-3″), 22.5 (C-17″), 14.0 (C-18″); ESI mass (negative mode): 443 $[M-H]^-$, 485 $[M + ACN]^-$.

4.5.6 *Geranylgeranyl ferulate (**12g**)*. White semi-solid,yield: 70 %; VLC mobile phase: *n*-hexan/ethyl acetate (8 : 2); ^{1}H NMR (500 MHz, $CDCl_3$): δ_H 7.61 (d, 1H, *J* = 16 Hz, H-3), 7.05 (dd, 1H, *J* = 1.6, 8 Hz, H-6′), 7.01 (d, 1H, *J* = 1.6, Hz, H-2′), 6.90 (d, 1H, *J* = 8, Hz, H-5′), 6.29 (d, 1H, *J* = 16 Hz, H-2), 5.43 (t, 2H, *J* = 7.0 Hz, H-2″), 5.09 (m, 1H, H-14″), 5.07 (4H, m, H-6″, H-10″), 4.70 (d, 2H, *J* =7.5 Hz, H-1″), 3.90 (s, 3H, OCH_3-3′), 2.16 (m, 2H, H-4″), 2.11(m, 2H, H-8″), 2.06 (m, 2H, H-12″), 1.98 (m, 6H, H-5″, H-9″, H-13″), 1.79 (s, 3H, H-20″), 1.67 (s, 3H, H-17″), 1.62 (s, 3H, H-16″), 1.59 (s, 6H, H-18″, H-19″); ^{13}C NMR (100 MHz, $CDCl_3$): δ_C 167.2 (C-1), 147.9 (C-3′), 146.7 (C-4′), 144.7

(C-3), 142.7 (C-3″), 135.8 (C-7″), 135.0 (C-11″), 131.2 (C-15″), 127.0 (C-1′), 124.4, 124.1 (C-6″, C-10″), 123.4 (C-14″), 123.0 (C-6′), 119.3 (C-2″), 115.6 (C-2), 114.7 (C-5′), 109.3 (C-2′), 61.0 (C-1″), 55.9 (OCH_3), 39.7 (C-5″, C-9″, C-13″), 32.2 (C-4″), 26.7, 26.6 (C-8″, C-12″), 25.7 (C-17″), 23.5 (C-20″), 17.6 (C-16″), 16.0 (C-18″, C-19″); ESI mass (negative mode): 465 $[M-H]^-$.

4.5.7 *2-Phenylethyl ferulate (**12h**)*. White semi-solid, yield: 67 %; Sephadex LH-20 (MeOH); ^1H NMR (400 MHz, $CDCl_3$): δ_H 7.68 (d, 1H, J = 15.6 Hz, H-3), 7.36 (m, 5H, H-4″-H8″), 7.11 (dd, 1H, J = 1.6, 8 Hz, H-6′), 7.09 (d, 1H, J = 1.6, Hz, H-2′), 6.99 (d, 1H, J = 8, Hz, H-5′), 6.35 (d, 1H, J = 15.6 Hz, H-2), 6.03 (s, 1H, OH), 4.50 (t, 2H, J = 6.8 Hz, H-1″), 3.90 (s, 3H, OCH_3-3′), 3.10 (t, 2H, J = 6.8 Hz, H-2″); ^{13}C NMR (100 MHz, $CDCl_3$): δ_C 167.2 (C-1), 148.0 (C-3′), 146.7 (C-4′), 144.9 (C-3), 137.9 (C-3″), 128.9 (C-4″, C8″), 128.5 (C-5″, C7″), 126.9 (C-1′), 126.5 (C-6″), 123.1 (C-6′), 115.3 (C-2), 114.7 (C-5′), 109.3 (C-2′), 64.8 (C-1″), 55.9 (OCH_3), 35.2 (C-2″); ESI mass (negative mode): 297 $[M-H]^-$.

4.5.8 *2-(p-Methylphenyl)ethyl ferulate (**12i**)*. White semi-solid, yield: 62 %; Sephadex LH-20 (MeOH); ^1H NMR (400 MHz, $CDCl_3$): δ_H 7.60 (d, 1H, J = 15.6 Hz, H-3), 7.15 (m, 4H, H-4″-H-5″, H-7″-H8″), 7.06 (dd, 1H, J = 1.6, 8.4 Hz, H-6′), 7.03 (d, 1H, J = 1.6, Hz, H-2′), 6.90 (d, 1H, J = 8.4, Hz, H-5′), 6.35 (d, 1H, J = 15.6 Hz, H-2), 5.86 (s, 1H, OH), 4.40 (t, 2H, J = 6.8 Hz, H-1″), 3.93 (s, 3H, OCH_3-3′), 3.0 (t, 2H, J = 6.8 Hz, H-2″), 2.30 (s, 3H, CH_3-6″); ^{13}C NMR (100 MHz, $CDCl_3$): δ_C 167.2 (C-1), 147.9 (C-3′), 146.7 (C-4′), 144.9 (C-3), 136.0 (C-3″), 134.8 (C-6″), 129.1 (C-5″, C7″), 128.5 (C-4″, C8″), 127.0 (C-1′), 123.1 (C-6′), 115.3 (C-2), 114.7 (C-5′), 109.3 (C-2′), 65.0 (C-1″), 55.9 (OCH_3), 34.8 (C-2″), 21.0 (CH_3); ESI mass (negative mode): 311 $[M-H]^-$.

4.5.9 *2-(o-Methylphenyl)ethyl ferulate (**12j**)*. White semi-solid, yield: 75 %; Sephadex LH-20 (MeOH); ^{1}H NMR (500 MHz, $CDCl_3$): δ_H 7.62(d, 1H, *J* = 15.6 Hz, H-3), 7.20 (m, 4H, H-5′-H8″), 7.07 (dd, 1H, *J* = 1.5, 8.4 Hz, H-6′), 7.03 (d, 1H, *J* = 1.5, Hz, H-2′), 6.90 (d, 1H, *J* = 8.4, Hz, H-5′), 6.29 (d, 1H, *J* = 15.6 Hz, H-2), 5.93 (s, 1H, OH), 4.40 (t, 2H, *J* = 7 Hz, H-1″), 3.92 (s, 3H, OCH_3-3′), 3.03 (t, 2H, *J* = 7 Hz, H-2″), 2.39 (s, 3H, CH_3-4″); ^{13}C NMR (100 MHz, $CDCl_3$): δ_C 167.2 (C-1), 148.0 (C-3′), 146.8 (C-4′), 144.9 (C-3), 136.4 (C-3″), 135.9 (C-4″), 130.3 (C-5″), 129.4 (C7″), 126.9 (C-1′), 126.7 (C-6″), 126.0 (C8″), 123.0 (C-6′), 115.4 (C-2), 114.7 (C-5′), 109.4 (C-2′), 64.0 (C-1″), 55.9 (OCH_3), 32.5 (C-2″), 19.4 (CH_3); ESI mass (negative mode): 311 $[M-H]^-$.

4.5.10 *2-(p-Chlorophenyl)ethyl ferulate (**12k**)*. White solid, yield: 62 %; m. p.: 53-54 °C; Sephadex LH-20 (MeOH); ^{1}H NMR (400 MHz, $CDCl_3$): δ_H 7.59 (d, 1H, *J* = 16 Hz, H-3), 7.27 (d, 2H, *J* = 8 Hz, H-5″, H-7″), 7.18 (d, 2H, *J* = 8 Hz, H-4″, H-8″), 7.05 (dd, 1H, *J* = 1.6, 8.4 Hz, H-6′), 7.02 (d, 1H, *J* = 1.6, Hz, H-2′), 6.91 (d, 1H, *J* = 8.4, Hz, H-5′), 6.26 (d, 1H, *J* = 16 Hz, H-2), 4.39 (t, 2H, *J* = 6.8 Hz, H-1″), 3.90 (s, 3H, OCH_3-3′), 2.98 (t, 2H, *J* = 6.8 Hz, H-2″); ^{13}C NMR (100 MHz, $CDCl_3$): δ_C 167.1 (C-1), 148.0 (C-3′), 146.8 (C-4′), 145.1 (C-3), 136.4 (C-3″), 132.3 (C-6″), 130.2 (C-5″, C-7″), 128.5 (C-4″, C-8″), 126.8 (C-1′), 123.0 (C-6′), 115.0 (C-2), 114.7 (C-5′), 109.4 (C-2′), 64.4 (C-1″), 55.9 (OCH_3), 34.5 (C-2″); ESI mass (negative mode): 331 $[M-H]^-$.

4.5.11 *2-(1-Naphthyl)ethyl ferulate (**12l**)*. Pale yellow solid, yield: 80 %; m. p.: 90-91 °C; VLC mobile phase: *n*-hexan/ethyl acetate (8.5 : 1.5); ^{1}H NMR (500 MHz, $CDCl_3$): δ_H 8.16 (d, 1H, *J* = 8.5 Hz, H-11″), 7.88 (br d, 1H, *J* = 8 Hz, H-8″), 7.78 (br d, 1H, *J* = 7 Hz, H-6″), 7.59 (d, 1H, *J* = 16 Hz, H-3), 7.57 (m, 1H, H-10″), 7.50 (m, 1H, H-9″), 7.40 (m, 2H, H-4″,H-5″), 7.06 (dd, 1H, *J* = 2, 8 Hz, H-6′), 7.01 (d, 1H, *J* = 2, Hz, H-2′), 6.92 (d, 1H, *J* = 8, Hz, H-5′), 6.29 (d, 1H, *J* = 16 Hz, H-2), 4.57 (t, 2H, *J* = 7.5 Hz, H-1″), 3.93 (s, 3H, OCH_3-3′), 3.51 (t, 2H, *J* = 7.5 Hz, H-2″); ^{13}C NMR (100 MHz,

$CDCl_3$): δ_C 167.2 (C-1), 148.0 (C-3′), 146.7 (C-4′), 145.0 (C-3), 133.8 (C-3″, C-7″), 132.1 (C-12″), 128.8 (C-8″), 127.4 (C-4″), 126.9 (C-1′, C-6″), 126.1 (C-10″), 125.6 (C-5″), 125.5 (C-11″), 123.7 (C-9″), 123.0 (C-6′), 115.3 (C-2), 114.7 (C-5′), 109.4 (C-2′), 64.4 (C-1″), 55.9 (OCH_3), 32.3 (C-2″); ESI mass (negative mode): 347 $[M-H]^-$.

4.6 General procedure for the synthesis of amide of ferulic acid **13f**

Ethyl chloroformate (0.76 mL, 8 mmol) and TEA (1.1 mL, 8 mmol) were added to a suspension of ferulic acid (0.737 g, 3.8 mmol) in DCM (10 mL) and stirred for 1 h at -15 °C until TLC analysis revealed a total consumption of starting material. Oleyl amine (17.4 mL, 80 mmol) and DMAP (0.030 g, 0.08 mmol) were then added and the mixture stirred at room temperature for 6 h. On completion, the solvent was evaporated *in vacuum*, and the crude product purified by Sephadex LH 20 with MeOH as eluent to give N-oleylferuloylamide (**13f**).

4.6.1 *N-oleylferulamide (**13f**)*. White solid, yield: 55%; m. p.: 50-51 °C; ^1H NMR (500 MHz, $CDCl_3$): δ_H 7.55 (d, 1H, J = 16 Hz, H-3), 7.05 (br d, 1H, J = 8 Hz, H-6′), 6.99 (br s, 1H, H-2′), 6.93 (d, 1H, J = 8, Hz, H-5′), 6.26 (d, 1H, J = 16 Hz, H-2), 5.74 (s, 1H, NH), 5.34 (m, 2H, H-9″, H-10″), 3.91 (s, 3H, OCH_3-3′), 3.37 (br s, 2H, H-1″), 2.0 (4H, H-8″, H11″), 1.56 (m, 2H, H-2″), 1.29 (m, 22H, H-3″-H-7″, H-12″-H17″), 0.88 (t, 3H, J = 7, Hz, H-18″); ^{13}C NMR (100 MHz, $CDCl_3$): δ_C 166.3 (C-1), 147.4 (C-3′), 146.7 (C-4′), 141.0 (C-3), 129.8 (C-10″), 129.7 (C-9″), 127.3 (C-1′), 122.0 (C-6′), 118.1 (C-2), 114.7 (C-5′), 109.7 (C-2′), 55.9 (OCH_3), 39.9 (C-1″), 32.6 (C-16″), 29.7, 29.6, 29.5, 29.4, 29.3, 29.2, (C-4″-C-7″, C-12″- C-15″), 28.2 (C-2″, C-3″), 27.0 (C-8″, C-11″), 22.7 (C-17″), 14.1 (C-18″); ESI mass (negative mode): 442 $[M-H]^-$.

4.7 General procedure for the synthesis of (*E*)-3,4-diethyloxycarbonyloxy caffeate **16f,g**

Ethyl chloroformate (1.52 mL, 16.7 mmol) and TEA (2.2 mL, 16 mmol) were added to a suspension of caffeic acid (0.737 g, 3.8 mmol) in DCM (10 mL) and stirred for 1 h at -15 °C until TLC analysis revealed a total consumption of starting material. Alcohol (8 mmol) and DMAP (0.030 g, 0.08 mmol) were then added and the mixture stirred at room temperature for 6 h. The solvent was evaporated under reduced pressure to afford the crude product. This product was purified by VLC (silica gel) using mixtures of *n*-hexane/ethyl acetate or toluene/ethyl acetate as eluents.

4.7.1 *Oleyl 3,4-diethyloxycarbonyloxy caffeate (**16f**)*. White solid, yield: 90%; VLC mobile phase: toluene/ethyl acetate (9.5 : 0.5); ^{1}H NMR (500 MHz, $CDCl_3$): δ_H 7.61 (d, 1H, J = 16 Hz, H-3), 7.45 (d, 1H, J = 2, Hz, H-2′), 7.4 (dd, 1H, J = 2, 8.5 Hz, H-6′), 7.30 (d, 1H, J = 8.5, Hz, H-5′), 6.38 (d, 1H, J = 16 Hz, H-2), 5.36 (m, 2H, H-9″, H-10″), 4.32 (q, 2H, J = 7.5 Hz, O$\underline{CH_2}$-CH_3), 4.33 (q, 2H, J = 7.5 Hz, O$\underline{CH_2}$-CH_3), 4.19 (t, 2H, J = 7 Hz, H-1″), 2.01 (4H, H-8″, H11″), 1.69 (m, 2H, H-2″), 1.39 (t, 6H, J = 7.5 Hz, OCH_2-$\underline{CH_3}$), 1.38 (t, 6H, J = 7.5 Hz, OCH_2-$\underline{CH_3}$), 1.31 (m, 2H, H-3″), 1.27 (20H, H-4″-H-7″, H-12″-H-17″), 0.88 (t, 3H, J = 7, Hz, H-18″).

4.7.2 *Geranylgeranyl 3,4-diethyloxycarbonyloxy caffeate (**16g**)*. White solid, yield: 87%; VLC mobile phase: toluene/ethyl acetate (9.5 : 0.5); ^{1}H NMR (500 MHz, $CDCl_3$): δ_H 7.62 (d, 1H, J = 16 Hz, H-3), 7.43 (d, 1H, J = 1.6, Hz, H-2′), 7.4 (dd, 1H, J = 1.6, 8.5 Hz, H-6′), 7.30 (d, 1H, J = 8.5, Hz, H-5′), 6.39 (d, 1H, J = 16 Hz, H-2), 5.42 (t, 2H, J = 7.0 Hz, H-2″), 5.13 (m, 1H, H-14″), 5.11 (4H, m, H-6″, H-10″), 4.70 (d, 2H, J =7 Hz, H-1″), 4.32 (q, 2H, J = 7.5 Hz, O$\underline{CH_2}$-CH_3), 4.33 (q, 2H, J = 7.5 Hz, O$\underline{CH_2}$-CH_3), 2.16 (m, 2H, H-4″), 2.12(m, 2H, H-8″), 2.07 (m, 2H, H-12″), 1.98 (m, 6H, H-5″, H-9″, H-13″), 1.79 (s, 3H, H-20″), 1.68 (s, 3H, H-17″), 1.62 (s, 3H, H-16″), 1.60 (s, 6H, H-18″, H-19″), 1.39 (t, 6H, J = 7.5 Hz, OCH_2-$\underline{CH_3}$), 1.38 (t, 6H, J = 7.5 Hz, OCH_2-$\underline{CH_3}$).

4.8 General procedure for the synthesis of caffeate **17f,g**

To a solution of the each protected caffeoyl ester **16f,g** (2.5 mmol) in DCM (10 mL) was added 80 equiv of piperidine (80 mmol) at 0 °C, and the reaction mixture was stirred at room temperature for 3h. The ester of caffeic acid was purified by VLC (silica gel) or Sephadex LH-20.

4.8.1 *Oleyl caffeate (**17f**)*. White solid, yield: 69%; m. p.: 68-69 °C; VLC mobile phase: *n*-hexane/ethyl acetate (7 : 3); ^{1}H NMR (500 MHz, $CDCl_3$): δ_H 7.59 (d, 1H, J = 16 Hz, H-3), 7.12 (d, 1H, J = 2, Hz, H-2′), 7.01 (dd, 1H, J = 2, 8.5 Hz, H-6′), 6.88 (d, 1H, J = 8.5, Hz, H-5′), 6.27 (d, 1H, J = 16 Hz, H-2), 6.18 (1H, OH), 5.93 (1H, OH), 5.34 (m, 2H, H-9″, H-10″), 4.20 (t, 2H, J = 7 Hz, H-1″), 2.01 (4H, H-8″, H11″), 1.70 (m, 2H, H-2″), 1.31 (m, 2H, H-3″), 1.29 (m, 4H, H-4″-H-5″), 1.27 (16H, H-6″, H-7″, H-12″-H-17″), 0.88 (t, 3H, J = 7, Hz, H-18″); ^{13}C NMR (100 MHz, $CDCl_3$): δ_C 168.1 (C-1), 146.4 (C-3′), 145.1 (C-3), 143.8 (C-4′), 130.0 (C-10″), 129.8 (C-9″), 127.5 (C-1′), 122.4 (C-6′), 115.6 (C-2′), 115.4 (C-2), 114.5 (C-5′), 65.0 (C-1″), 31.9 (C-16″), 29.8, 29.7, 29.5, 29.4, 29.3, 29.2, (C-4″-C-7″, C-12″- C-15″), 28.8 (C-2″), 27.2, 27.1 (C-8″, C-11″), 26.0 (C-3″), 22.7 (C-17″), 14.1 (C-18″); ESI mass (negative mode): 429 $[M-H]^-$.

4.8.2 *Geranylgeranyl caffeate (**17g**).* White solid, yield: 55 %; m. p.: 53-54 °C; Sephadex LH-20 (MeOH); ^{1}H NMR (500 MHz, $CDCl_3$): δ_H 7.59 (d, 1H, J = 16 Hz, H-3), 7.09 (d, 1H, J = 1.6, Hz, H-2′), 6.98 (dd, 1H, J = 1.6, 8.5 Hz, H-6′), 6.87 (d, 1H, J = 8.5, Hz, H-5′), 6.26 (d, 1H, J = 16 Hz, H-2), 6.0 (s, 1H, OH), 5.43 (t, 2H, J = 7.0 Hz, H-2″), 5.13 (m, 1H, H-14″), 5.09 (4H, m, H-6″, H-10″), 4.69 (d, 2H, J =7 Hz, H-1″), 2.16 (m, 2H, H-4″), 2.12 (m, 2H, H-8″), 2.07 (m, 2H, H-12″), 1.98 (m, 6H, H-5″, H-9″, H-13″), 1.79 (s, 3H, H-20″), 1.68 (s, 3H, H-17″), 1.61 (s, 3H, H-16″), 1.59 (s, 6H, H-18″, H-19″); ^{13}C NMR (100 MHz, $CDCl_3$): δ_C 167.1 (C-1), 146.3 (C-3′), 144.8 (C-3), 143.8 (C-4′), 142.8 (C-3″), 135.9 (C-7″), 135.0 (C-11″), 131.3 (C-15″), 127.6 (C-1′), 124.4, 124.2 (C-6″, C-10″),

123.4 (C-14″), 122.4 (C-6′), 119.1 (C-2″), 115.7 (C-2′), 115.5 (C-2), 114.4 (C-5′), 61.3 (C-1″), 39.7 (C-5″, C-9″, C-13″), 32.2 (C-4″), 26.8, 26.6 (C-8″, C-12″), 25.7 (C-17″), 23.6 (C-20″), 17.7 (C-16″), 16.0 (C-18″, C-19″); ESI mass (negative mode): 465 $[M-H]^-$.

4.8 General procedure for the synthesis of N-oleylcaffeamide **18f**

Ethyl chloroformate (1.52 mL, 16.7 mmol) and TEA (2.2 mL, 16 mmol) were added to a suspension of caffeic acid (0.737 g, 3.8 mmol) in DCM (10 mL) and stirred for 1 h at -15 °C until TLC analysis revealed a total consumption of starting material. Oleyl amine (17.4 mL, 80 mmol) and DMAP (0.030 g, 0.08 mmol) were then added and the mixture stirred at room temperature for 6 h. On completion, the solvent was evaporated *in vacuo*, and the crude product purified by Sephadex LH 20 with MeOH as eluent to give N-oleylcaffeamide (**18f**).

4.8.1 *N-oleylcaffeamide (**18f**)*. White solid; yield: 75%; m. p.: 68-69 °C; ^{1}H NMR (500 MHz, $CDCl_3$): δ_H 7.49 (d, 1H, J = 15.5 Hz, H-3), 7.11 (br s, 1H, H-2′), 6.85 (m, 1H, H-6′), 6.81 (d, 1H, J = 8, Hz, H-5′), 6.40 (s, 1H, OH), 6.24 (d, 1H, J = 15.5 Hz, H-2), 5.36 (m, 2H, H-9″, H-10″), 3.34 (br s, 2H, , H-1″), 1.99 (4H, H-8″, H11″), 1.55 (m, 2H, H-2″), 1.26 (22 H, H-3″- H-7″, H-12″-H-17″), 0.88 (t, 3H, J = 6.5, Hz, H-18″); ^{13}C NMR (100 MHz, $CDCl_3$): δ_C 167.9 (C-1), 147.0 (C-3′), 144.4 (C-3), 142.7 (C-4′), 129.9 (C-10″), 129.8 (C-9″), 126.8 (C-1′), 121.5 (C-6′), 116.5 (C-2′), 115.5 (C-2), 114.7 (C-5′), 40.4 (C-1″), 31.9 (C-16″), 29.8, 29.7, 29.5, 29.4, 29.3, 29.2, (C-2″-C-7″, C-12″- C-15″), 27.2, 27.1 (C-8″, C-11″), 22.7 (C-17″), 14.1 (C-18″); ESI mass (negative mode): 428 $[M-H]^-$.

4.9 Molecular Modeling

Ligand **18f** was docked considering the global minimum energy conformation and the conformations within 5 kcal/mol and with different RMSD values from the global minimum as determined by molecular mechanics conformational analysis performed with Macromodel software [39]. In practical, theoretical 3D model of the compound was built by means of Maestro GUI. The molecule was then submitted to a conformational search of 1000 steps with an energy window for saving structure of 21 kJ/mol (5.02 kcal/mol). The algorithm used was the Monte Carlo method followed by an energy minimization carried out using the MMFFs [40], the GB/SA water implicit solvation model [41] and the Polak-Ribier Coniugate Gradient (PRCG) method for 5000 iterations, converging on gradient with a threshold of 0.05 kJ(molÅ)$^{-1}$.

4.9.1 Docking

The docking experiments were performed as described in our previous works [30, 31] applying QM-Polarized Ligand Docking (QMPLD) [36]. In order to better take into account the induced fit phenomena, the most energy favoured generated complexes were fully optimized using AMBER* united atoms force field [42] in GB/SA implicit water [41], setting 10000 steps interactions analysis with Polak-Ribier Coniugate Gradient (PRCG) method and a convergence criterion of 0.1 kJ/(molÅ). The resulting complexes were considered for the binding modes graphical analysis with Pymol [43] and Maestro [44].

4.10. Biochemistry studies

4.10.1 Expression and purification of recombinant HIV-1 RT

HIV-1 RT group M subtype B. Heterodimeric RT was expressed essentially as described [30]. Briefly, E. coli strain M15 containing the p6HRT-prot vector was grown to an optical density at 600

nm of 0.7 and induced with 1.7 mM isopropyl β-D-1-thiogalactopyranoside (IPTG) for 4 h. Protein purification was carried out with a BioLogic LP system (Biorad), using a combination of immobilized metal affinity and ion exchange chromatography. Cell pellets were resuspended in lysis buffer (50 mM sodiumphosphate buffer pH 7.8, containing 0.5 mg/mL lysozyme), incubated on ice for 20 min, and after adding NaCl to a final concentration of 0.3 M, were sonicated and centrifuged at 30,000×g for 1 h. The supernatant was loaded onto a Ni2+-NTA-Sepharose column pre-equilibrated with loading buffer (50 mM sodium phosphate buffer pH 7.8, containing 0.3M NaCl, 10% glycerol, and 10 mM imidazole) and washed thoroughly with wash buffer (50 mM sodium phosphate buffer pH 6.0, containing 0.3 M NaCl, 10% glycerol, and 80 mM imidazole). RT was eluted with an imidazole gradient in wash buffer (0 – 0.5 M). Fractions were collected, protein purity was checked by SDS-PAGE and found to be higher than 90%. The 1:1 ration between the p66/p51 subunits was also verified. Enzyme-containing fractions were pooled and diluted 1:1 with 50 mM sodium phosphate buffer pH 7.0, containing 10% glycerol; and then loaded into a Hi-trap heparin HP GE (Healthcare Lifescience) pre-equilibrated with 10 column volumes of loading buffer(50 mM sodium phosphate buffer pH 7.0, containing 10% glycerol and 150 mM NaCl). The column was then washed with loading buffer and the RT was eluted with Elute Buffer 2 (50 mM Sodium Phosphate pH 7.0, 10% glycerol, 1 M NaCl). Fractions were collected, protein was dialyzed and stored in buffer containing 50 mM TrisHCl pH 7.0, 25 mM NaCl, 1mM EDTA, and 50% glycerol. Catalytic activities and protein concentrations were determined. Enzyme-containing fractions were pooled and aliquots were stored at −80 ◦C.

4.10.2 HIV-1 DNA polymerase-independent RNase H activity determination

HIV RT-associated RNase H activity was measured as described [45] using the RNase H inhibitor RDS1759 [30] as a control. In 100 µL reaction volume containing 50 mM Tris-HCl buffer pH 7.8, 6 mM MgCl2, 1 mM dithiothreitol (DTT), 80 mM KCl, 0.25 µM hybrid RNA/DNA 5'-

GAUCUGAGCCUGGGAGCU-Fluorescin-3' (HPLC, dry, QC: Mass Check) (available from Metabion)5'-Dabcyl-AGCTCCCAGGCTCAGATC-3'(HPLC, dry, QC: Mass Check), increasing concentrations of inhibitor, whose dilution were made in water, and 20 ng of wt RT according to a linear range of dose-response curve. The reaction mixture was incubated for 1 h at 37 °C, stopped by addition of EDTA and products were measured with a multilabel counter plate reader Victor 3 (Perkin Elmer model 1420-051) equipped with filters for 490/528 nm (excitation/emission wavelength).

4.10.3 HIV-1 RNA-dependent DNA polymerase activity determination

RNA-dependent DNA polymerase (RDDP) activity was measured as described [46] using the NNRTI Efavirenz as a control. in 25 µL volume containing 60 mM Tris-HCl buffer pH 8.1, 8 mM MgCl2, 60 mM KCl, 13 mM DTT, 2.5 µM poly(A)-oligo(dT),100 µM dTTP, increasing concentrations of inhibitor, whose dilution were made in water, and 6 ng of wt RT according to a linear range of dose-response curve. After enzyme addition, the reaction mixture was incubated for 30 min at 37 °C and the stopped by addition of EDTA. Reaction products were detected by picogreen addition and measured with a multilabel counter plate reader Victor 3 (Perkin Elmer model 1420-051) equipped with filters for 502/523 nm (excitation/emission wavelength).

4.10.4 The Yonetani-Theorell analysis

The Yonetani-Theorell analysis was performed as described previously [38, 47].

4.10.5 Isobologram analysis.

The isobologram analysis was carried out as previously described [48].

ACKNOWLEDGMENT

This Article is based upon work from COST Action CA15135, supported by COST.

Author Contributions

The manuscript was written through contributions of all authors. All authors have given approval to the final version of the manuscript.

Supplementary data. Supplementary data associated with this article: ^{1}H and ^{13}C NMR spectra of the final compounds. Supplementary material associated with this article can be found, in the online version, at …

References

[1] P. Zahn, C. Pannecouque, E. De Clercq, X. Liu, Anti-HIV drug discovery and devolopment: current innovations and future trends, J. Med. Chem. 59, (2016) 2301-2311.

[2] L., Menèndes-Arias, Molecular basis of immunodeficiency virus type 1 drug resistance; overview and recent developments, Antiviral Res. 98, (2013) 93-120.

[3] S.F.J. Le Grice, Human immunodeficiency virus reverse transcriptase: 25 years of research, drug discovery, and promise, J. Biol. Chem. 287, (2012) 40850-40857

[4] A. Corona, F. Esposito, E. Tramontano,. Can the ever-promising target HIV reverse transcriptase-associated RNase H become a success story for drug development?, Future Virol. 9,(2014) 448-445.

[5] A. Corona, T. Masaoka, G. Tocco, E. Tramontano, S.F.J.Le Grice, Active site and allosteric inhibitors of the ribonuclease H activity of HIV reverse transcriptase, Future Med. Chem. 5, (2013) 2127-2139.

[6] F. Esposito, E. Tramontano, Past and future. Current drugs targeting HIV-1 integrase and Reverse Transcriptase-Associated Ribonuclease H activity: single and dual active site inhibitors, Antivir. Chem. Chemother. 23, (2014) 129-144.

[7] S. Distinto, E. Maccioni, R. Meleddu, A. Corona, S.Alcaro, E. Tramontano, Molecular aspects of the RT/drug interactions. Perspective of dual inhibitors, Curr. Pharm. Des. 19, (2013) 1850-1859.

[8] F. Esposito, C. Sanna, C. Del Vecchio, V. Cannas, A. Venditti, A. Corona, A. Bianco, A.M. Serrilli, L. Guarcini, C. Parolin, M. Ballero, E. Tramontano,.*Hypericum hircinum* L. components as new single-molecule inhibitors of both HIV-1 reverse transcriptase-associated DNA polymerase and ribonuclease H activities, Pathog. Dis. 68, (2013) 116-124.

[9] F. Esposito, I. Carli, C. Del Vecchio, L. Xu, A. Corona, N. Grandi, D. Piano, E. Maccioni, S. Distinto, C. Parolin, E. Tramontano, Sennoside A, derived from the traditional chinese medicine plant *Rheum* L., is a new dual HIV-1 inhibitor effective on HIV-1 replication, Phytomedicine 23, (2016), 1383-1391

[10] S. Mondal, B.R. Mirdha, S.C. Mahapatra, The science behind sacredness of Tulsi (*Ocimum sanctum* Linn.), Indian J. Physiol. Pharmacol. 53, (2009) 291-306.

[11] M.M. Cohen, Tulsi - *Ocimum sanctum*: A herb for all reasons, J. Ayurveda Integr. Med. 5 (2014) 251-259.

[12] A.A. Rege, R.Y. Ambaye, R.A. Deshmukh, *In-vitro* testing of anti-HIV activity of some medicinal plants, Indian J. Nat. Prod. Resour. 1, (2010) 193-199.

[13] P. R. Usha, M. U. R. Naidu, Y. S. N. Raju, Evaluation of the antiretroviral activity of a new polyherbal drug (Immu-25) in patients with HIV infection, Drugs R.D. 4, (2003) 103-109.

[14] S. Ruiu, N. Anzani, A. Orrù, C. Floris, P. Caboni, S. Alcaro, E. Maccioni, S. Distinto, F. Cottiglia, Metoxyflavones from *Stachys glutinosa* with binding affinity to opioid receptors: *In silico*, *in vitro* and *in vivo* study, J. Nat. Prod. 78, (2015) 69-76.

[15] C. Peng, G. Bodenhausen, S. Qiu, H.H.S. Fong, N.R. Farnsworth, S. Yuan, C. Zheng, Computer-assisted structure elucidation: application of CISOC–SES to the resonance assignment and structure generation of betulinic acid, Magn. Reson. Chem. 36, (1998) 267-278.

[16] W. Seebacher, N. Simic, R. Weis, R. Saf, O. Kunert, Complete assignments of ^{1}H and ^{13}C NMR resonances of oleanolic acid, 18α-oleanolic acid, ursolic acid and their 11-oxo derivatives. Magn. Reson. Chem. 41, (2003) 636-638.

[17] J.-J. Cheng, L.-J. Zhang, H.-L. Cheng, C-T. Chiou, I-J. Lee, Y.-H. Kuo. Cytotoxic hexacyclic triterpene acids from *Euscaphis japonica*, J. Nat. Prod. 73, (2010) 1655–1658.

[18] J.L.C. Wright, A.G. McInnes, S. Shimizu, D.G. Smith, J.A. Walter, D. Idler, W. Khalil, Identification of C-24 alkyl epimers of marine sterols by ^{13}C nuclear magnetic resonance spectroscopy. Can. J. Chem. 56, (1978) 1898-1903.

[19] A.F. Erasmuson, R. J. Ferrier, N. C. Franca, H. E. Gottlieb, E. Wenkert, ^{13}C Nuclear magnetic resonance spectroscopy of vanillin derivatives, J. Chem. Soc. Perkin I **(**1977) 492-494.

[20] H. H. Barakat, M.A.M. Nawwar, J. Buddrus, M. Linscheid. Niloticol, A phenolic glyceride and two phenolic aldehydes from the roots of *Tamarix nilotica*, Phytochemistry, 26**, (**1987) 1837-1838.

[21] A.E. Nkengfack, T.W. Vouffo, J.C. Vardamides, J. Kouam, Z.T. Fomum, M. Meyer, O. Sterner, Phenolic metabolites from *Erythrina species*, Phytochemistry 46, (1997) 573-578.

[22] K. Nakamura, T. Nakajima, T. Aoyama, S. Okitsu, M. Koyama, One-pot esterification and amidation of phenolic acids, Tetrahedron 70, (2014) 8097-8107.

[23] A. Corona, F.S. Di Leva, S. Thierry, L. Pescatori, G. Cuzzucoli Crucitti, F. Subra, O. Delelis, F. Esposito, G. Rigogliuso, R. Costi, S. Cosconati, E. Novellino, R. Di Santo, E. Tramontano, Identification of highly conserved residues involved in inhibition of HIV-1 RNase H function by diketo acid derivatives. Antimicrob. Agents Chemother. 58, (2014) 6101-6110.

[24] T. Akihisa, J. Ogihara, J. Kato, K. Yasukawa, M. Ukiya, S. Yamanouchi, K. Oishi, Inhibitory Effects of Triterpenoids and Sterols on Human Immunodeficiency Virus-1 Reverse Transcriptase. Lipids 36, (2001) 507-512.

[25] J. Zhang, X. Liu, E. De Clercq, Capsid (CA) protein as a novel drug target: recent progress in the research of HIV-1 CA inhibitors, Mini Rev. Med. Chem. 9, (2009) 510-518.

[26] M. Estrada, C. Herrera-Arozamena, C. Pérez, D. Viña, A. Romero, J. A. Morales-García, A. Pérez-Castillo, M. I. Rodríguez-Franco, New cinnamic e *N*-benzylpiperidine and cinnamic e *N*,*N*-dibenzyl(*N*-methyl)amine hybrids as Alzheimer-directed multitarget drugs with antioxidant, cholinergic, neuroprotective and neurogenic properties, Eur. J. Med. Chem. 121, (2016) 376-386.

[27] Z. Chen, M. Digiacomo, Y. Tu, Q. Gu, S. Wang, X. Yang, J. Chu, Q. Chen, Y. Han, J. Chen, G. Nesi, S. Sestito, M. Macchia, S. Rapposelli, R. Pi, Discovery of novel rivastigmine-hydroxycinnamic acid hybrids as multi-targeted agents for Alzheimer's disease, Eur. J. Med. Chem. 125, (2017) 784-792.

[28] S. Ruiu, N. Anzani, A. Orrù, C. Floris, P. Caboni, E. Maccioni, S. Distinto, S. Alcaro, F. Cottiglia, N-Alkyl dien- and trienamides from the roots of *Otanthus maritimus* with binding affinity for opioid and cannabinoid receptors, Bioorg. & Med. Chem. 21, (2013) 7074-7082.

[29] K.A. Paris, O. Haq, A.K. Felts, K. Das, E. Arnold, R.M. Levy, Conformational landscape of the Human Immunodeficiency Virus Type 1 reverse transcriptase non-ncleoside inhibitor binding pocket: Lessons for inhibitor design from a cluster analysis of many crystal structures, J. Med. Chem., 52, (2009) 6413-6420.

[30] A. Corona, R. Meleddu, F. Esposito, S. Distinto, G. Bianco, T. Masaoka, E. Maccioni, L. Menéndez-Arias, S. Alcaro, S.F.J. Le Grice, E. Tramontano, Ribonuclease H/DNA polymerase HIV-1 reverse transcriptase dual inhibitor: Mechanistic studies on the allosteric mode of action of isatin-based compound RMNC6, PLoS ONE, 11 (2016) e0147225.

[31] R. Meleddu, V. Cannas, S. Distinto, G. Sarais, C. Del Vecchio, F. Esposito, G. Bianco, A. Corona, F. Cottiglia, S. Alcaro, C. Parolin, A. Artese, D. Scalise, M. Fresta, A. Arridu, F. Ortuso, E. Maccioni, E. Tramontano, Design, synthesis, and biological evaluation of 1,3-diarylpropenones as dual inhibitors of HIV-1 reverse transcriptase, ChemMedChem, 9 (2014) 1869-1879.

[32] J. Barnett-Norris, F. Guarnieri, D.P. Hurst, P.H. Reggio, Exploration of biologically relevant conformations of anandamide, 2-arachidonylglycerol, and their analogues using conformational memories, J. Med. Chem., 41 (1998) 4861-4872.

[33] N. Sauton, D. Lagorce, B.O. Villoutreix, M.A. Miteva, MS-DOCK: Accurate multiple conformation generator and rigid docking protocol for multi-step virtual ligand screening, BMC Bioinformatics, 9 (2008) 1-12.

[34] D. Plewczynski, M. Łaźniewski, R. Augustyniak, K. Ginalski, Can we trust docking results? Evaluation of seven commonly used programs on PDBbind database, J. Computat. Chem. 32, (2011) 742-755.

[35] E. Perola, W.P. Walters, P.S. Charifson, A detailed comparison of current docking and scoring methods on systems of pharmaceutical relevance, Proteins: Struct. Funct. Bioinf. 56 (2004) 235-249.

[36] Schrödinger LLC., QMPolarized protocol, Schrodinger Suite New York, NY, USA.

[37] D.M. Himmel, S.G. Sarafianos, S. Dharmasena, M.M. Hossain, K. McCoy-Simandle, T. Ilina, A.D.Jr. Clark, J. L. Knight, J.G. Julias, P.K. Clark, K. Krogh-Jespersen, R.M, Levy, S.H. Hughes, M. A. Parniak, E, Arnold, HIV-1 reverse transcriptase structure with RNase H inhibitor dihydroxy benzoyl naphthyl hydrazone bound at a novel site, ACS Chem. Biol. 20, (2016) 702-712.

[38] T. Yonetani, The Yonetani-Theorell graphical method for examining overlapping subsites of enzyme active centers, Methods Enzymol. 87, (1982) 500–509.

[39] F. Mohamadi, N.G.J. Richards, W.C. Guida, R. Liskamp, M. Lipton, C. Caufield, G. Chang, T. Hendrickson, W.C. Still, Macromodel-an integrated software system for modeling organic and bioorganic molecules using molecular mechanics, J. Comput. Chem. 11, (1990) 440-467.

[40] T. Halgren, Merck molecular force field. II. MMFF94 van der Waals and electrostatic parameters for intermolecular interactions, J. Comput. Chem. 17, (1996) 520-552.

[41] W.C. Still, A. Tempczyk, R.C. Hawley, T. Hendrickson, Semianalytical treatment of solvation for molecular mechanics and dynamics, J. Amer. Chem. Soc. 112, (1990) 6127-6129.

[42] D.Q. McDonald, W.C. Still, AMBER torsional parameters for the peptide backbone. Tetrahedron Lett. 33, (1992) 7743-7746.

[43] PyMOL, Molecular Graphics System Schrödinger, LLC.

[44] Schrödinger LLC., Maestro GUI, New York, NY, USA, 2013.

[45] G. Cuzzucoli Crucitti, M. Métifiot, L. Pescatori, A. Messore, V. N. Madia, G. Pupo, F. Saccoliti. L. Scipione, S. Tortorella, F. Esposito, A. Corona, M. Cadeddu, C. Marchand, Y. Pommier, E. Tramontano, R. Costi, R. Di Santo, Structure-activity relationship of pyrrolyl diketo acid derivatives as dual inhibitors of HIV-1 integrase and reverse transcriptase ribonuclease H domain, J. Med. Chem. 58, (2015) 1915-1928.

[46] L. Xu, N. Grandi, C. Del Vecchio, D. Mandas, A. Corona, D. Piano, F. Esposito, C. Parolin, E. Tramontano, From the traditional Chinese medicine plant *Schisandra chinensis* new scaffolds effective on HIV-1 reverse transcriptase resistant to non-nucleoside inhibitors, J. Microbiol. 53, (2015) 288-293.

[47] R. Meleddu, S. Distinto, A. Corona, G. Bianco, V. Cannas, F. Esposito, A. Artese, S. Alcaro, P. Matyus, D. Bogdan, F. Cottiglia, E. Tramontano, E. Maccioni, (3Z)-3-(2-[4-(aryl)-1,3-thiazol-2-yl]hydrazin-1-ylidene)-2,3-dihydro-1H-indol-2-one derivatives as dual inhibitors of HIV-1 reverse transcriptase, Eur. J. Med. Chem. 93, (2015) 452–460.

[48] A.C. Tintori, A. Corona, F. Esposito, A. Brai, E.R. Ceresola, M. Clementi, F. Canducci, M. Botta, Inhibition of HIV-1 Reverse Transcriptase Dimerization by Small Molecules, ChemBioChem 17, (2016) 683–688.